Chandra Data Analysis Coordinate Systems: Rev 6.0.2

SDS-2.0

Jonathan McDowell

2024 Mar 27

Contents

List of Tables

List of Figures

1 General Introduction

This document describes the coordinate systems used for Chandra data analysis. It partly supersedes the 1999 document 'ASC Coordinate Systems, Rev 5.0' but omits some of the details in that document.

The document attempts to put Chandra data-analysis in a relatively abstract, that is to say mission-independent, framework. No discussion is made of the spacecraft coordinate system used for the mechanical engineering aspects of the mission, or of the coordinate systems for the aspect camera.

After a short discussion of the pixel convention, we set the context by giving in section 2 an overview of the main coordinate systems used for looking at ACIS imaging data. In section 3, we present a detailed mission-independent model of coordinate systems, and in section 4 we return to the details of Chandra-specific analysis as implemented within that mission-independent framework.

1.1 Pixel convention

Summary: (256.0, 256.0) represents the center of a pixel whose lower left corner is (255.5, 255.5).

In all cases where we use discrete, integer-valued, **pixel numbers**, the corresponding real-valued, continuous **pixel coordinates** are defined to be equal to the pixel number at the center of the pixel. We further recommend that for finite detector planes, one corner be designated as the lower left corner, LL. Then the pixel which has LL as one of its corners (i.e. the lower left pixel) shall be numbered (1,1) so that its center has coordinates (1.0, 1.0). The coordinates of the LL point itself are (0.5, 0.5). If the detector is rectangular with sides of length XMAX, YMAX the pixel coordinates then run from (0.5, 0.5) in the lower left corner (LL) to (XMAX+0.5, YMAX+0.5) in the upper right corner (UR) while the pixel numbers in each axis run from 1 to XMAX, 1 to YMAX.

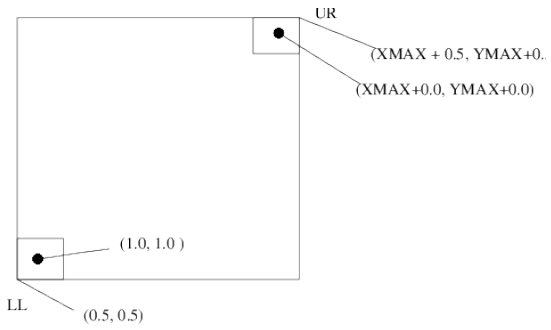

Figure 1: Pixel convention.

See the appendix for further notational conventions.

2 Overview of Data Analysis Coordinates

Summary: A photon from (RA, Dec) enters the mirror at (Theta, Phi) and hits the detector at (CCD_ID, CHIPX, CHIPY).

We pixelize these image planes thus: the photon comes from pixel SKY(X,Y), enters the mirror at DET(DETX,DETY) and hits chip CCD_ID at CHIP(CHIPX, CHIPY).

Astronomers expect to image their data in celestial coordinates - potentially equatorial, galactic or some other system, but we shall assume equatorial ICRS RA and Dec is the system of interest. In a conventional optical telescope with rigid pointing the resulting tangent plane image is the same as that created on the detector. In an X-ray telescope, however, spacecraft dither, geometric effects and other effects mean that the image on the detector plane is quite different from the sky image, and is related to it in a complicated time-dependent way. Therefore, it can be useful to make separate images in celestial coordinates, mirror-centered coordinates, and instrument coordinates - they do not look the same and show different information.

In Chandra data analysis, we often must relate a detected event at a particular location on a detector chip to a photon celestial location in ICRS RA and Dec, or simulate the predicted chip location given the RA and Dec of a source. To do this, we represent the different steps in the process of observing the photon with different coordinate systems.

Paired with the conceptual coordinate frames in physical units, we define pixel tangent planes used to make the software images in that coordinate frame.

In this section we give a simplified overview of an ACIS imaging observation.

2.1 Chip pixel coordinates

The raw data telemetered from Chandra is in terms of the event positions on the chip, and can be represented in **chip coordinates**. For ACIS the pixel numbers run from 1 to 1024 along CHIPX and CHIPY. Floating-point chip coordinates, specifying sub-pixel locations, run from (0.5, 0.5) (lower left) to (1024.5,1024.5) (upper right).

In the case of ACIS the chip coordinates corresponding to actual physical hardware pixels. Other detectors, such as HRC, may not have actual hardware pixels.

Because of the spacecraft dither, a point source in the sky describes a Lissajous figure in chip coordinates - in practice an edge-brightened square, as seen in the figure. You might think this ruins the point of having a high spatial resolution telescope, but we have the arrival times of each photon, so we can reconstruct the original celestial positions of those photons to high accuracy in subsequent steps.

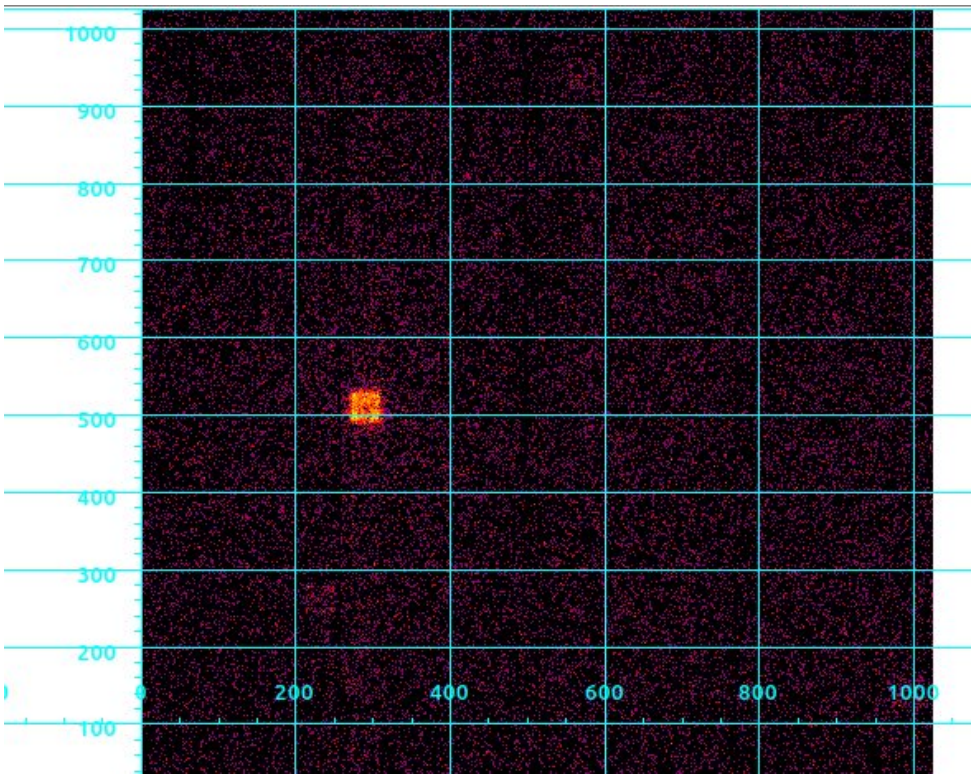

Figure 2: ACIS image, chip pixels. Single chip, with coords running from 0.5 to 1024.5 on each axis.

The chip coordinates CHIPX,CHIPY don't specify a unique location - if you take an event file and make a CHIPX vs CHIPY image all the chips will lie on top of each other. We can separate them by using the chip number CCD_ID, which for ACIS runs from 0 to 9.

2.2 Chip physical coordinates

Along with the chip coordinates we define linear **chip physical coordinates** (CPC) representing the actual physical distance in mm from the chip lower left corder.

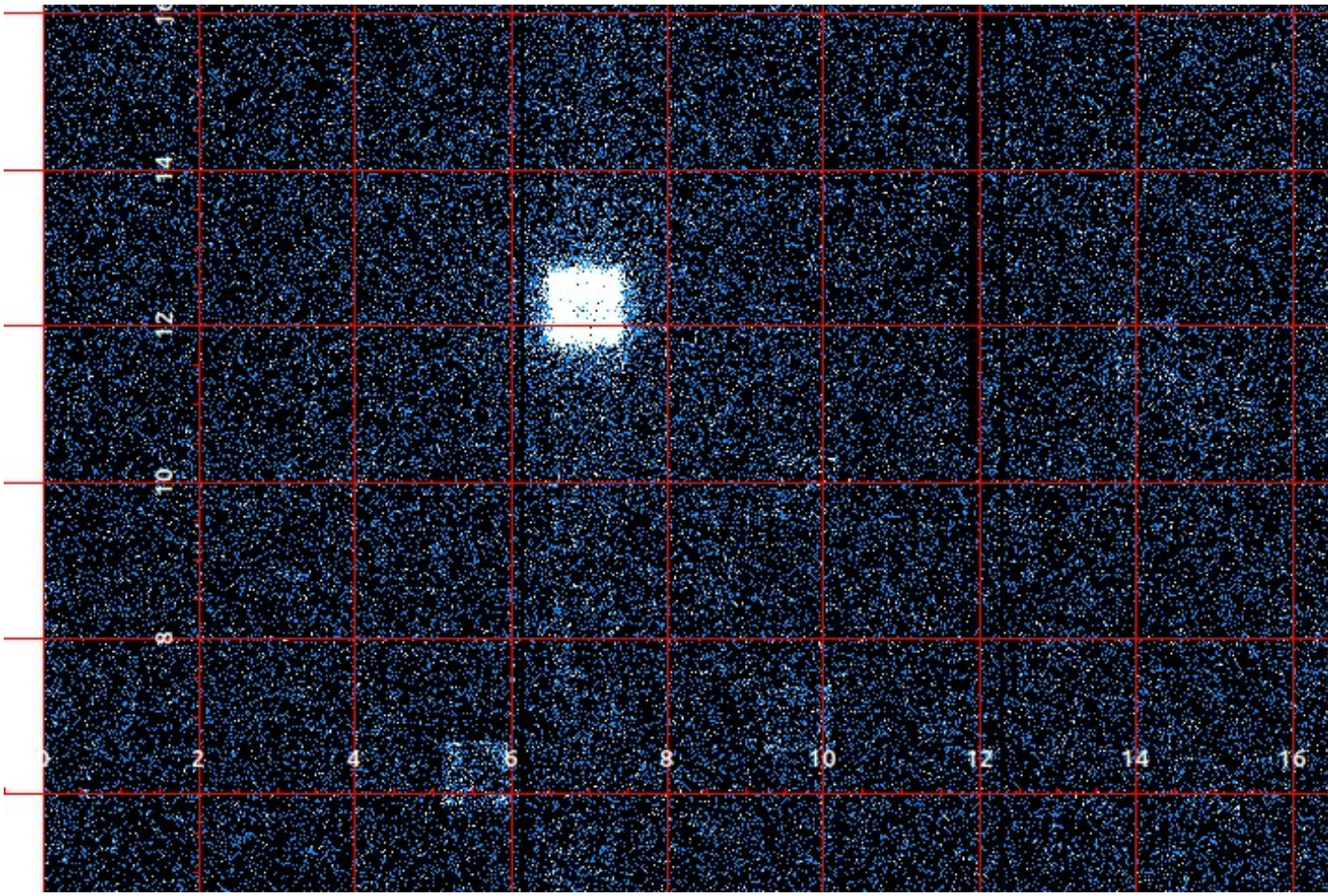

Figure 3: ACIS image, chip pixels - CPC coordinates running from 0 to 24.58mm on each axis

An additional system, TDET (tiled detector coordinates) was provided to set the chips out in a fictitious flat plane without overlapping. TDET is mostly used for creating weighted exposure maps via the sky2tdet program.

2.3 Off-axis Angle coordinates

Given the SIM X (focus) and SIM Z (translation) values in mm, and the 3D coordinates of the corners of each detector chip, we can now map the triple (CCD_ID, CHIPX, CHIPY) to a three-dimensional position in the spacecraft relative to the telescope optical axis.

We define **mirror Spherical Coordinates** to be the off-axis angle THETA from a nominal (as calibrated) optical axis, and an azimuth angle PHI relative to the HRMA Y axis. We usually represent theta in armin and phi in degrees.

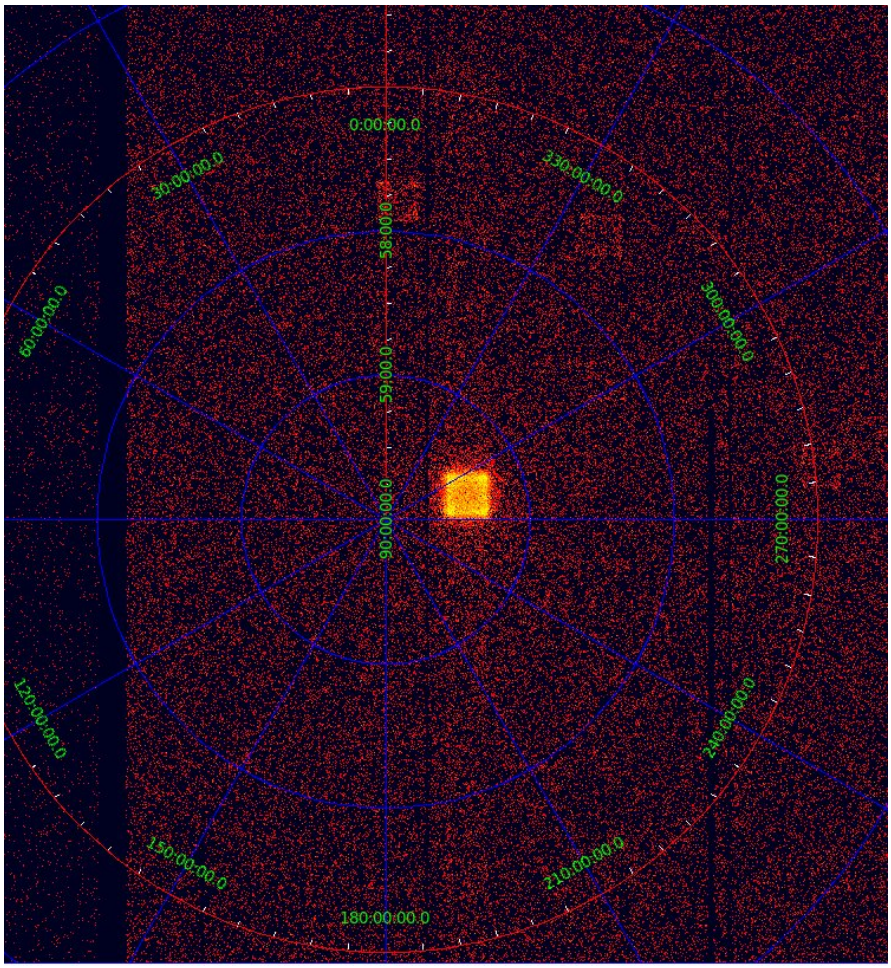

Figure 4: ACIS image, mirror spherical coordinates. Fixed in the mirror, optical axis at centre of field

2.4 Detector pixel coordinates

For analysis we lay down a pixel plane, the (misnamed in a misguided attempt at ROSAT back compatibility) **detector coordinate** pixel system. It is a tangent plane to the sky as seen in optical-axis-centered coordinates. For ACIS, the tangent point coordinates are (4096.5, 4096.5).

These detector pixel coordinates are labelled DET(DETX,DETY) in the files. Vignetting and mirror sensitivity functions are specified in this frame, using this coord system or the off-axis-angle system.

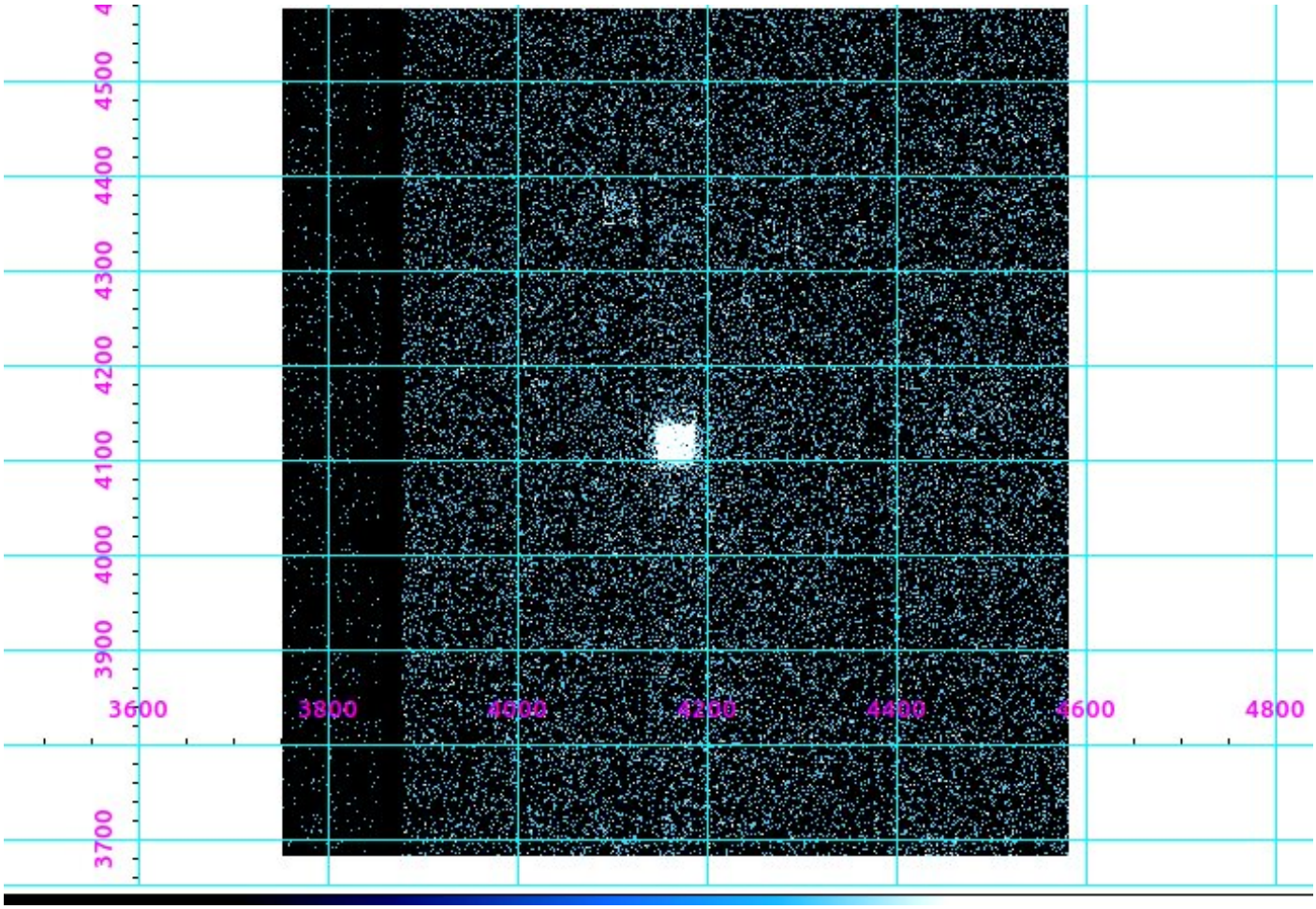

Figure 5: ACIS image, detector pixels. Fixed in the mirror, with the optical axis at (4096.5, 4096.5)

2.5 Celestial Coordinates

At a given moment, a photon arrives at the Chandra aperture from a given ICRS RA and Dec - the **celestial coordinates**.

Normally when we do science we want to think of the image in **celestial coordinates**, RA (α) and Dec (δ), in degrees. Loading a Chandra event file into DS9 and selecting `analysis->coordinate grid` will show these celestial coordinates by default.

The mirror spherical coordinates map to the celestial coordinates in a **time dependent way** during an observation because of dither, although sometimes for low accuracy work we use a mean pointing to make an approximate mirror-to-sky correspondence.

This time-dependent mapping is called the **aspect solution**, implemented as a file containing the optical axis coordinates and spacecraft roll angle versus time. The event files contain the CHIP and DET coordinates centered in the chip and the mirror as well as the calculated SKY coordinates representing the celestial position.

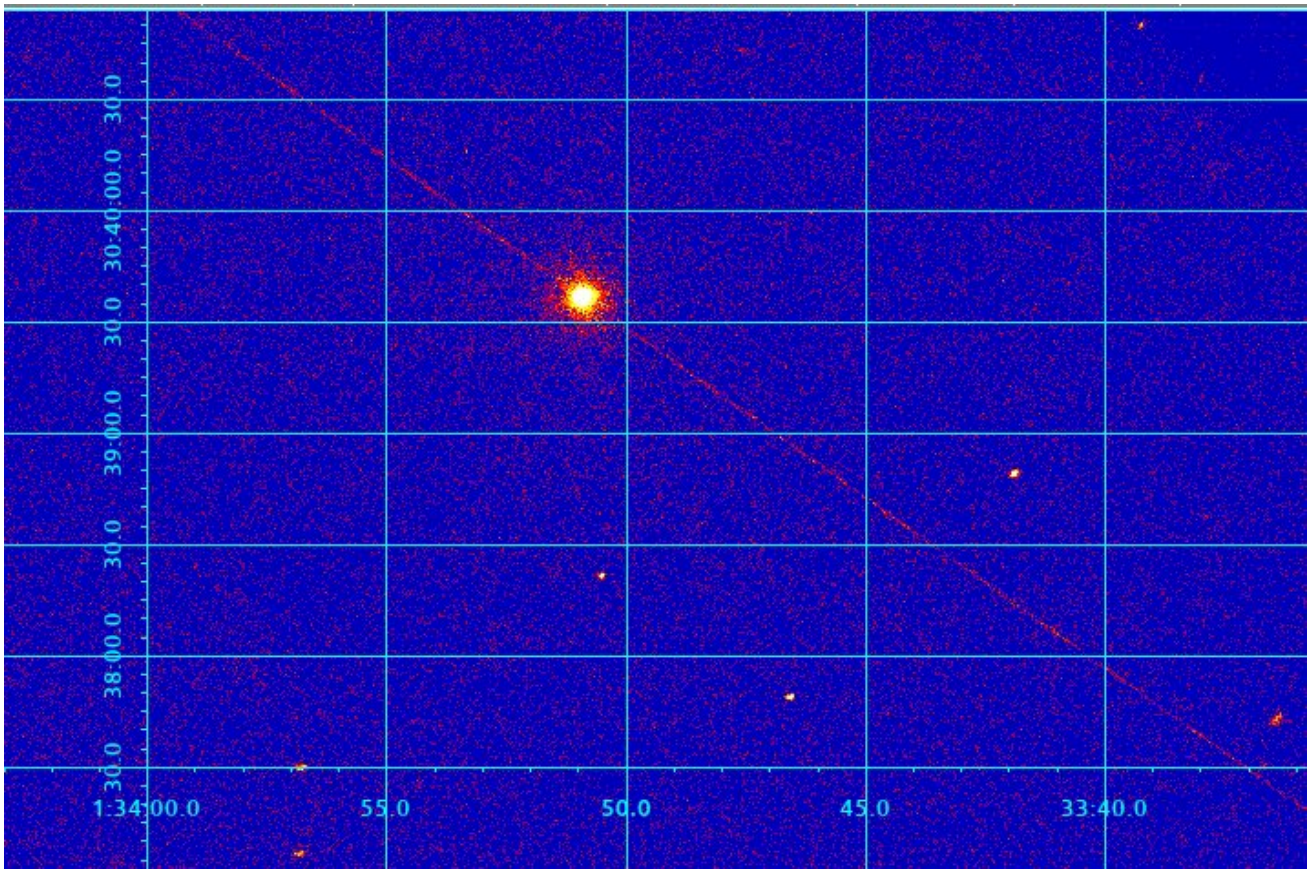

Figure 6: ACIS image, celestial coordinate grid. Fixed in the sky, with center at the nominal (usually mean-of-aspect-solution) RA and Dec of the observation.

2.6 Sky Pixel Coordinates

The pixel plane system corresponding to the celesital coordinates is called **sky coordinates**, given as SKY(X,Y) in the data files.

To perform actual analysis we project the celestial positions onto a tangent plane centered at the mean nominal pointing direction of the telescope (not exactly equal to the true optical axis due to calibration limitations). We lay down a finite pixel plane (**sky coordinates** on this tangent plane with a Y axis pointing to celestial north. In the case of ACIS this plane runs from 0.5 to 8192.5 in X and Y and so is centered at (4096.5, 4096.5) which coincides with the nominal pointing direction.

DS9 will convert between this system ('physical' in DS9 terms) and celestial coordinates ('WCS' in DS9 terms) on the fly, and display the cursor values of both in its info panel.

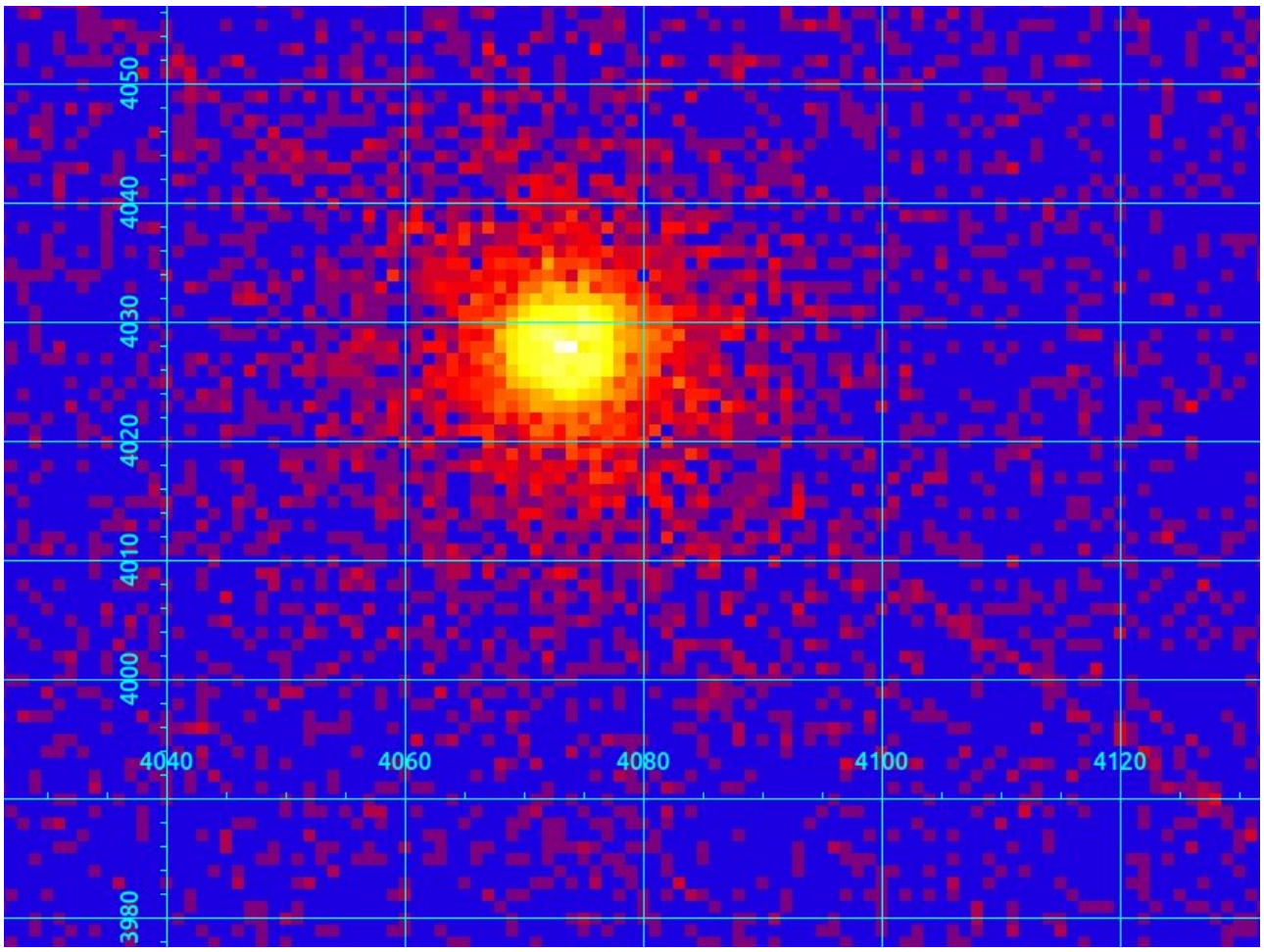

Figure 7: ACIS image, sky pixels. Nominal pointing direction is at pixel (4096.5,4096.5).

3 Mission-independent formulation

3.1 Data Analysis Coordinate Systems - Imaging

3.1.1 General model of the system

The system we describe is:

- **Observatory**, consisting of several
- **Telescopes**. Each telescope has a
- **Mirror** (or optical system, more generally) which images the sky by converting incoming photon paths to outgoing photon paths in a well determined way, and an
- **Instrument compartment** located near the focus of the optics, with an
- **Instrument table** on which are mounted one or more
- **Instruments**.

  The instruments are assumed to be fixed with respect to the instrument table, but the table may move relative to the instrument compartment. (So, the distances between different instruments are fixed). An additional degree of freedom is that the instrument compartment itself may move relative to the optical system (this degree of freedom is not present for the Chandra flight spacecraft, but did exist in the ground calibration setup). Each instrument consists of one or more fixed
- **Chips** - rectangular planar detector surfaces of finite area; our term is not meant to imply that they are chips in the semiconductor sense.

  Note that physical detector plane may not be rectangular (e.g. ROSAT PSPC); this can be handled by setting the sensitivity of the remaining part of the plane to zero.

  Each chip is subdivided into rectangular (usually square) 'detector pixels';
- **Detector pixels** enumerate the set of distinct locations that can be represented in the instrument telemetry stream. In the case of CCDs, these correspond to physical CCD pixels, while in microchannel plate detectors they are arbitrarily set by the electronics.

The information available to us, the telemetry position, is two dimensional, but to infer the final two dimensional angular incoming sky direction we must calculate a photon position in three dimensional space. Every time we want to make an image, we use a two dimensional pixel plane (possibly losing information in a third dimension). So the three types of coordinate system we will use are:

- Two dimensional pixel plane
- Two dimensional spherical angular coordinates
- Three dimensional cartesian coordinates.

3.2 Data Analysis 1: Telemetry to Tangent Plane

Once instrumental details are removed, we derive the CHIP pixel coordinate system which records a location in a 2-dimensional plane pixel surface. The FP (Focal Plane) pixel coordinate system (called DETX,DETY in the FITS files) gives the locations in a pixelized tangent plane to the telescope optical axis. The SKY (X,Y) pixel coordinate system gives locations in a pixelized tangent plane to the nominal RA and Dec of observation. Going from CHIP to FP involves taking out 3-D geometry of the chips, position of the instrument on the optical bench, motion of the optical bench, boresights, and plate scale. Going from FP to SKY involves applying the aspect solution. These three pixel coordinate systems are the systems that users will see in data analysis. In addition, the TDET system, which combines the CHIP systems for all the components of one detector and systems associated with dispersive gratings, is present in the event files.

The remaining coordinate systems are used internally to make precise the transformations involved in going from CHIP to FP to SKY.

3.2.1 Telemetry to Chip coordinates

The telemetry coordinates of a photon are a collection (n-tuple) of integers. The formats may be very different from instrument to instrument; for instance, the HRC telemetry coordinates consist of two Tap values and six voltages, while the ACIS telemetry coordinates are directly given as pixel numbers. For each instrument, we provide a rule to convert from telemetry coordinates to our standard data analysis **chip pixel coordinates** which run from 1 to XMAX, 1 to YMAX. They define a logical plane extending from coordinate 0.5 to XMAX+0.5, 0.5 to YMAX+0.5. In other words, the center of pixel number (1,1) is (1.0, 1.0), and its lower left corner is (0.5, 0.5). The logical plane may be larger than the actual set of possibly active pixels. For instance, for a circular detector such as the ROSAT PSPC, we extend this logical chip pixel coordinate plane to be rectangular.

The corresponding physical coordinate system is a three dimensional Cartesian system called **Chip Physical Coordinates (CPC)**, giving the physical location of a detected photon event on the active area surface. They are fully defined in terms of the chip pixel coordinates when the pixel size Δ_p and the array size XMAX x YMAX is given, although they are specific to a single chip of the multi-chip array.

$(X_{CPC}, Y_{CPC}, Z_{CPC})$ are defined to have units of mm. The CPC X and Y axes are coincident with the chip X and Y axes, and the Z axis completes a right handed set. The CPC Z coordinate

of any point in the chip has a value of 0.0. The X and Y coordinates run from 0.0 to XLEN and YLEN, where $XLEN = XMAX * \Delta_p$ and $YLEN = YMAX * \Delta_p$.

Thus if a photon lands at Chip Physical Coordinates X_{CPC}, Y_{CPC} its chip pixel coordinates are

$$\begin{aligned} CHIPX &= X_{CPC}/\Delta_p + 0.5 \\ CHIPY &= Y_{CPC}/\Delta_p + 0.5 \end{aligned} \tag{1}$$

or

$$\begin{aligned} X_{CPC} &= (CHIPX - 0.5)\Delta_p \\ Y_{CPC} &= (CHIPY - 0.5)\Delta_p \end{aligned} \tag{2}$$

Note that CHIPX and CHIPY are by definition linear, by which I mean that the mapping to real physical space is linear. Now for ACIS it so happens that the true CCD pixels satisfy this condition sufficiently accurately, but for HRC the readout values require linearization and removal of discontinuities.

3.2.2 Tiled Detector Coordinates

In an instrument with multiple detector planes, the planes may be tilted with respect to each other, or may be separated by a non-integral number of detector pixels, or both (as in ACIS-I). Projecting onto a 2-D plane (e.g. FP coords) will then lose the identity of individual pixels since one true detector pixel will map to a variable number of square pixels on the projected plane. For recording calibration information like bad pixel lists and inspecting the raw image, it may be useful to have a single coordinate system covering the whole instrument which retains true detector pixel identity at the expense of relative positional accuracy. For this purpose we introduced the tiled detector coordinate systems (TDET). However, users mostly don't deal with the TDET system except for certain exposure map cases.

$$\begin{pmatrix} TDETX \\ TDETY \end{pmatrix} = \Delta_i \begin{pmatrix} 1 & 0 \\ 0 & H_i \end{pmatrix} \begin{pmatrix} \cos\theta_i & \sin\theta_i \\ -\sin\theta_i & \cos\theta_i \end{pmatrix} \begin{pmatrix} CHIPX - 0.5 \\ CHIPY - 0.5 \end{pmatrix} + \begin{pmatrix} X0_i + 0.5 \\ Y0_i + 0.5 \end{pmatrix} \tag{3}$$

where the values of H_i, Δ_i and θ_i are different for each chip. H_i gives the handedness of the planar rotation and has values $+1$ or -1, Δ_i gives the sub-pixel resolution factor, and θ_i gives the rotation angle of the chip axes with respect to the detector coordinate axes.

The TDET parameters for tiled detector coordinates are arbitrary, so there can be several parallel TDET systems for one instrument and individual TDET labels assigned for each system must be used.

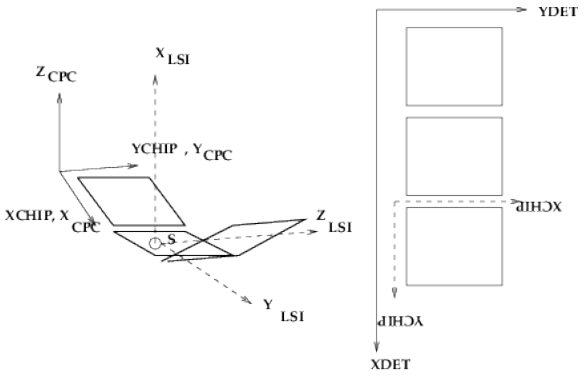

Figure 8: The relationship between CHIP and Tiled Detector coordinates.

3.2.3 Local Science Instrument coordinates

Each instrument has an Instrument Origin which is the nominal focal point for the instrument. For telescopes with movable instrument tables, the actual focal point for a particular observation may be different.

To describe the motion of the instrument table, we use three aligned Cartesian coordinate systems.

- The Science Instrument Translation Frame (STF) coordinate system is fixed in the instrument compartment, and is used to describe the changing position of the instrument table. Its origin is at the flight focus and its axes have +X running from the focus toward the telescope aperture, and +Y and +Z forming a right handed set whose orientation matches that of the observatory coordinates. For AXAF, the direction of instrument table motion is along Z.

- The Science Instrument Translation Table (STT) coordinate system is fixed in the moving instrument table, and is used to describe the positions of the instrument origins relative to each other. The position of its origin is mission-dependent, but the axes are parallel to the STF axes.

- The Local Science Instrument (LSI) coordinate system for each instrument is fixed in that instrument, and is identical to the STT frame but with the origin shifted to the instrument origin.

When the instrument table is moved to put the instrument at its nominal focus position, that means that the LSI origin is coincident with the STF origin. Since the axes are also parallel, STF and LSI coordinates become identical. The STF system therefore measures how much the instrument is offset from its nominal focus.

The STF, LSI and STT coordinate systems are defined to use units of mm. To convert from the LSI system to the STT system, one needs to know the STT coordinates of each LSI origin (i.e.

the location of each instrument on the instrument table). To convert to the STF system, one needs to know the instantaneous position of the instrument table, which we describe by giving the STF coordinates of the STT origin O_{STT}.

To convert from a position P(LSI) in LSI coords to P(STF) in STF coords, one then performs the vector sum:

$$P(STF) = P(LSI) + O_{LSI}(STT) + O_{STT}(STF) \tag{4}$$

adding the STT coordinates of the LSI origin and the STF coordinates of the STT origin. When the instrument is at its nominal focus, these two vectors are equal and opposite.

To convert from CPC coordinates to LSI coordinates, we need to carry out a rotation and translation. Each instrument has one LSI coordinate system, and several chips each with its own CPC system. The information we need for each chip to define the transformation is the LSI coordinates of each of the four corners of the chip plane (actually, only three of the four are required).

A general point on the plane is

$$\boldsymbol{r} = \boldsymbol{p_0} + X_{CPC}\boldsymbol{e}_X + Y_{CPC}\boldsymbol{e}_Y \tag{5}$$

where $\boldsymbol{p_0}$ is the origin of CPC coordinates, and $\boldsymbol{e}_X$ and $\boldsymbol{e}_Y$ are the unit vectors along the CPC axes, with $\boldsymbol{e}_Z$ as the unit normal to the plane.

Let us denote the position vectors of the four chip corners as $\boldsymbol{LL}$,$\boldsymbol{UL}$,$\boldsymbol{UR}$,$\boldsymbol{LR}$. Then the unit vectors of the CPC origin and axes in LSI coordinates are

$$\boldsymbol{p_0} = \boldsymbol{LL}, \boldsymbol{e}_X = \boldsymbol{LR} - \boldsymbol{LL}, \boldsymbol{e}_Y = \boldsymbol{UL} - \boldsymbol{LL} \tag{6}$$

and

$$\boldsymbol{e}_Z = \boldsymbol{e}_X \wedge \boldsymbol{e}_Y. \tag{7}$$

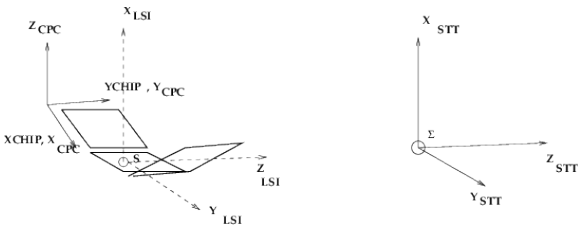

Figure 9: The relationship between CHIP, LSI and STT coordinates.

We can recast this in a rotational formulation,

$$P_G(LSI) = P_{LL}(LSI) + R(CPC, LSI)P_G(CPC) \tag{8}$$

where the matrix is

$$R(CPC, LSI) = \begin{pmatrix} (\boldsymbol{e_X})_X & (\boldsymbol{e_Y})_X & (\boldsymbol{e_Z})_X \\ (\boldsymbol{e_X})_Y & (\boldsymbol{e_Y})_Y & (\boldsymbol{e_Z})_Y \\ (\boldsymbol{e_X})_Z & (\boldsymbol{e_Y})_Z & (\boldsymbol{e_Z})_Z \end{pmatrix} \tag{9}$$

These unit axis vectors can easily be derived from the corner coordinates.

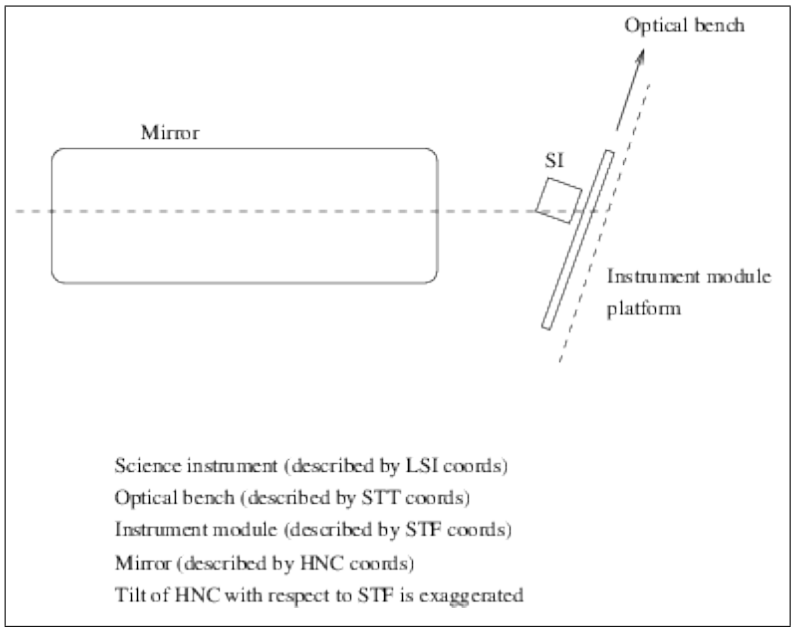

Figure 10: The instrument compartment (dashed line) may be misaligned with the telescope mirrors. At calibration, this misalignment (highly exaggerated here) may be significant and variable as the mirror is tilted with respect to the instruments. The instrument bench moves with respect to the instrument compartment, as indicated by the arrow.

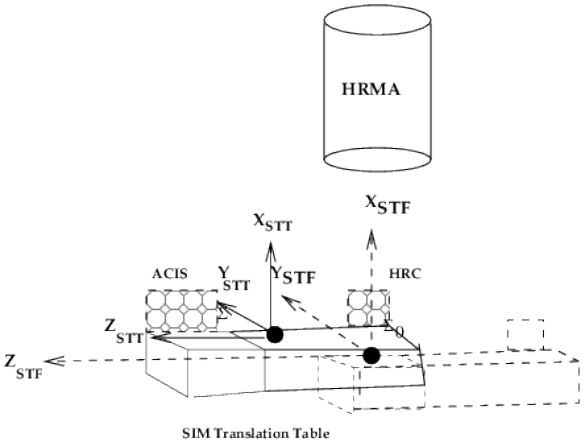

Figure 11: The relationship between STT and STF coordinates, AXAF example. The instrument (SIM) table has moved so that HRC is at the focus.

3.2.4 Mirror coordinates

We now specialize to a simple optical system which can be modelled to first order as a thin lens with an optical node N from which rays appear to emerge toward a detector. This simple description is fine for the AXAF HRMA, but won't apply directly to the complicated optical path of the AXAF Aspect Camera. The origin of mirror coordinates (labelled here as MNC for Mirror Nodal Coordinates, in previous versions of the document HNC for HRMA Nodal Coordinates) is the nominal optical node of the mirrors. The +X axis goes from the node toward the entrance aperture, and the Y and Z axes complete a right handed system. To first order, an incoming ray with MNC direction cosines $(-X_N, Y_N, Z_N)$ emerges from the mirror with direction cosines $(-X_N, -Y_N, -Z_N)$. (We use the subscript 'N' for mirror nodal coordinates).

The mirror has a nominal focal length f, and a nominal focus at mirror coordinates (-f, 0, 0). We define Focus Coordinates (FC-1.0) as a cartesian system identical to MNC coordinates but with its origin at the focus. Thus

$$P(MNC) = (-f, 0, 0) + P(FC) \tag{10}$$

The nominal connection between FC and STF coordinates is

$$P(FC) = P(STF) \tag{11}$$

However, we support the more general alignment

$$P(FC) = O_{STF}(FC) + R(STF, FC)P(STF). \tag{12}$$

This equation allows us to handle systems in which the instrument compartment can move relative to the mirror system, for example the inversion of the HRMA with respect to the instrument compartment that was originally planned for Chandra ground calibration.

Associated with the MNC system are two spherical coordinate systems. Mirror Spherical Coordinates measure the off axis angle and azimuth of an incoming ray, and their pole is the MNC $+X_N$ axis. Focal Surface Coordinates measure the off axis angle and azimuth of an emerging ray, with pole at the $-X_N$ axis (toward the focus). Each of these spherical coordinate systems has an associated family of pixel plane coordinate systems (parameterized by the selected pixel size), tangent to the pole of the sphere.

The generic Focal Plane Pixel coordinates are

$$\begin{aligned} FPX &= FPX0 + t_x \Delta_s^{-1}(Y_N/|X_N|) \\ FPY &= FPY0 + t_y \Delta_s^{-1}(Z_N/|X_N|) \end{aligned} \tag{13}$$

where t_x, t_y are sign parameters which control the orientation of the image. Δ_s is the pixel size in radians. The actual physical pixel size at the focus, for focal length f, is

$$\Delta_p = f\Delta_s \tag{14}$$

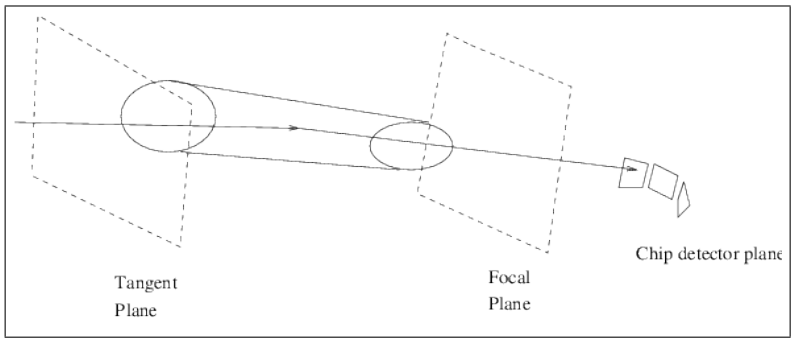

Figure 12: The Tangent Plane Coordinate system describes the incoming rays, while the Focal Plane Coordinates system describes the angular position of rays emerging from the mirrors. The rays then intersect one of several inclined detector planes, causing events whose locations are described in tiled detector coordinates.

A focal plane pixel coordinate system is defined in terms of this physical pixel size. The nominal focal length of the mirror is then needed to convert to actual angular size. (In practice, the angular size may be directly encoded in a WCS CDELT header parameter).

The Tangent Plane pixel coordinates are defined in the same way, but form the pixel plane for the Mirror Spherical Coordinates. Specifically, we define the standard **ASC-FP-FSC-1.0** variant of focal plane coordinates as $(t_x = 1, t_y = -1)$

$$\begin{aligned} FPX &= FPX0 + \Delta_s^{-1}(Y_N/|X_N|) \\ FPY &= FPY0 - \Delta_s^{-1}(Z_N/|X_N|) \end{aligned} \tag{15}$$

Note that in the focal plane X_N is negative but we take the absolute value in the formula. The sign on FPY is then chosen to take out the mirror inversion of the image caused by the optics. The sign on FPX reflects the fact that we want celestial longitude to increase from right to left when the roll angle is zero.

To repeat this in another way: (assuming zero roll angle and the default chip orientation)

- Source moves to higher RA
- Source moves to left in sky image, so sky X decreases
- FPX decreases
- Incoming photon moves to smaller MNC Y and MNC Y/$|X|$
- Image moves to larger MNC Y, FC Y, LSI Y, CHIP X

and

- Source moves to higher Dec
- Source moves up in sky image, so sky Y increases
- FPY increases
- Incoming photon moves to larger MNC Z
- Image moves to smaller MNC Z, FC Z, LSI Z, CHIP Y

We define the standard version of tangent plane coordinates as

$$\begin{aligned} TPX &= FPX0 + \Delta_s^{-1}(Y_N/|X_N|) \\ TPY &= FPY0 - \Delta_s^{-1}(Z_N/|X_N|) \end{aligned} \tag{16}$$

(identical to the focal plane coordinates) where here the (X_N, Y_N, Z_N) are the unit vector in MNC coordinates of the incoming ray. Tangent plane coordinates are defined to apply to positions on the 'sky' side of the mirror, and do not include mirror optical distortions, while focal plane coordinates do. In practice we assume that tangent plane and focal plane coordinates are identical, and mirror distortions are handled in the spatial variation of the centroid of the PSF.

Thus in our simple mirror model where an incoming photon coming from unit vector (X, Y, Z) with ray unit vector $(-X, -Y, -Z)$ is imaged to a ray with the same unit vector $(-X, -Y, -Z)$, the tangent plane coordinates of the incoming photon TPX, TPY are equal to the focal plane coordinates of the imaged ray. For incoming rays the sign of X is always negative, so -X is positive.

We define Mirror Spherical Coordinates (r, θ_H, ϕ_H) in terms of mirror nodal Cartesian coordinates as follows:

$$\begin{pmatrix} X_N \\ Y_N \\ Z_N \end{pmatrix} = \begin{pmatrix} rcos\theta_H \\ r\sin\theta_H\cos\phi_H \\ r\sin\theta_H\sin\phi_H \end{pmatrix} \tag{17}$$

The angle θ_H is the **MSC off-axis angle** and ϕ_H is the **MSC Azimuth**. The inverse is

$$\begin{aligned} r &= \sqrt{X_N^2 + Y_N^2 + Z_N^2} \\ \theta_H &= \cos^{-1}(X_N/r) \\ \phi_H &= \arg(Y_N, Z_N) \end{aligned} \tag{18}$$

The Focal Surface Coordinates (r, θ_F, ϕ_F) are

$$\begin{pmatrix} X_N \\ Y_N \\ Z_N \end{pmatrix} = \begin{pmatrix} -rcos\theta_F \\ r\sin\theta_F\cos\phi_F \\ r\sin\theta_F\sin\phi_F \end{pmatrix} \tag{19}$$

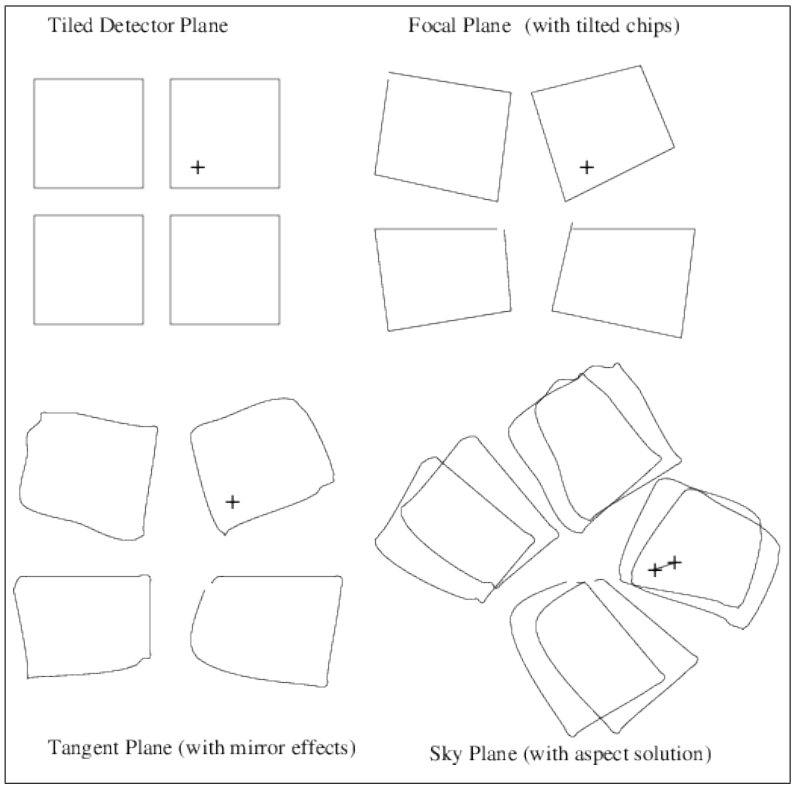

Figure 13: The different pixel plane coordinate systems. Distorting effects are highly exaggerated.

The angle θ_F is the **FSC off-axis angle** and the angle ϕ_F is the **FSC azimuth**. They are related to the MSC coordinates by

$$\theta_F = \pi - \theta_H, \quad \phi_F = \phi_H \tag{20}$$

The inverse is

$$\begin{aligned} r &= \sqrt{X_N^2 + Y_N^2 + Z_N^2} \\ \theta_H &= \cos^{-1}(-X_N/r) \\ \phi_H &= \arg(Y_N, Z_N) \end{aligned} \tag{21}$$

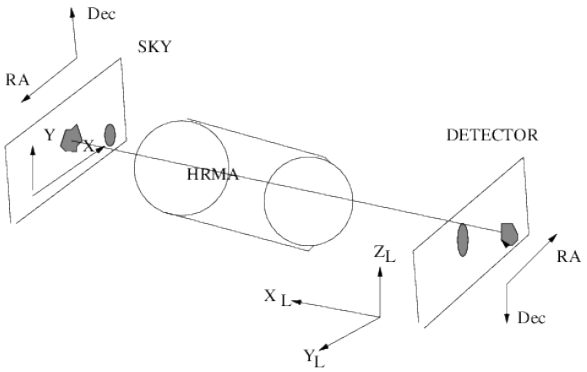

Figure 14: Imaging the sky in LSI coordinates

3.3 Data Analysis 2: Tangent Plane to Sky

3.3.1 Sky Pixel Coordinates

The Sky Pixel coordinate system is a translation and rotation of the Tangent Plane pixel coordinate system to align the image with a nominal pointing direction and spacecraft roll angle. For small aspect corrections, sky pixel coordinates are

$$\begin{aligned} X &= FPX0 + (TPX - FPX0)\cos\gamma - (TPY - FPY0)\sin\gamma + A_X \\ Y &= FPY0 + (TPX - FPX0)\sin\gamma + (TPY - FPY0)\cos\gamma + A_Y \end{aligned} \tag{22}$$

The quantities A_X and A_Y are the sky frame aspect offsets in pixels, determining the sky pixel coordinates of the optical axis. (Note that the aspect offsets for Einstein and Rosat were stored as detector frame offsets, which required applying the roll angle to; it's not clear to me why this choice was made.)

In general when combining data over a wide range of pointing directions, (mosaicing images) we must reproject to the nominal sky tangent plane.

3.3.2 Physical Tangent Plane coordinates

If the Tangent Plane pixel coordinates represent a position on the tangent plane to the unit sphere at the optical axis, the Physical Tangent Plane coordinate system

$$\begin{pmatrix} X_{PTP} \\ Y_{PTP} \\ Z_{PTP} \end{pmatrix} = \begin{pmatrix} -\Delta_s(TPX - TPX0) \\ \Delta_s(TPY - TPY0) \\ 1 \end{pmatrix}. \tag{23}$$

represents the 3D vector from the center of the unit sphere to that position on the tangent plane, which the convention that the X_{PTP} and Y_{PTP} axes run in the direction of increasing RA and Dec respectively in the on-orbit case with zero roll. The PTP system is closely related to HRMA Nodal coordinates. If the direction of the incoming ray is (X_N, Y_N, Z_N) then

$$\begin{pmatrix} X_{PTP} \\ Y_{PTP} \\ Z_{PTP} \end{pmatrix} = \begin{pmatrix} Y_N/X_N \\ Z_N/X_N \\ 1 \end{pmatrix} \tag{24}$$

3.3.3 Physical Sky Plane coordinates

The Physical Sky Plane coordinate system for zero aspect offset and finite roll angle is

$$\begin{pmatrix} X_{PSP} \\ Y_{PSP} \\ Z_{PSP} \end{pmatrix} = \begin{pmatrix} X_{PTP}\cos\gamma + Y_{PTP}\sin\gamma \\ X_{PTP}\sin\gamma - Y_{PTP}\cos\gamma \\ Z_{PTP} \end{pmatrix} \tag{25}$$

where γ is the spacecraft roll angle.

The PTP and PSP systems are important as you need them to calculate the RA and Dec. However they are only used in internal calculations.

3.3.4 J2000 Celestial Coordinates

One can go from Tangent Plane Physical coordinates to J2000 celestial coordinates using the instantaneous pointing direction (α_A, δ_A). and roll angle γ_A.

$$\mathcal{S}(\alpha, \delta) = \mathrm{Rot}(\pi/2 + \gamma_A, \pi/2 - \delta_A, \pi - \alpha_A) \begin{pmatrix} X_{PTP} \\ Y_{PTP} \\ Z_{PTP} \end{pmatrix} \tag{26}$$

Use the nominal pointing direction (α_0, δ_0) and set the roll angle to zero if using Sky Plane Physical Coordinates:

$$\mathcal{S}(\alpha, \delta) = \mathrm{Rot}(\pi/2, \pi/2 - \delta_0, \pi - \alpha_0) \begin{pmatrix} X_{PSP} \\ Y_{PSP} \\ Z_{PSP} \end{pmatrix} \tag{27}$$

From TP pixel coordinates, recall that

$$\begin{pmatrix} X_{PTP} \\ Y_{PTP} \\ Z_{PTP} \end{pmatrix} = \begin{pmatrix} -\Delta_s(TPX - TPX0) \\ \Delta_s(TPY - TPY0) \\ 1 \end{pmatrix} \tag{28}$$

3.4 Simulation: Sky to Telemetry

3.4.1 Mirror Spherical Coordinates to Focal Surface Coordinates

Incoming photons with given mirror spherical coordinates (off axis angle and azimuth) can be described by their tangent plane pixel coordinates. To first order, these are the same as the focal plane pixel coordinates; determining the higher order corrections is the job of ray trace simulators such as SAOSAC. When simulating, we often will not bother with these tangent and pixel plane coordinates but instead will work directly with mirror nodal coordinates.

3.4.2 Focal Surface or Mirror Nodal Coordinates to CPC coordinates

We then have the problem: how to transform from mirror nodal coordinates of a ray emerging from the mirror to the detected photon position. This is harder than working in the data analysis direction. We choose a Cartesian coordinate system (usually LSI coordinates) and calculate the intersection of the ray line with each detector plane. There should be only one detector plane which has an intersection within its finite bounds (i.e., the photon will only hit one of the chips). For

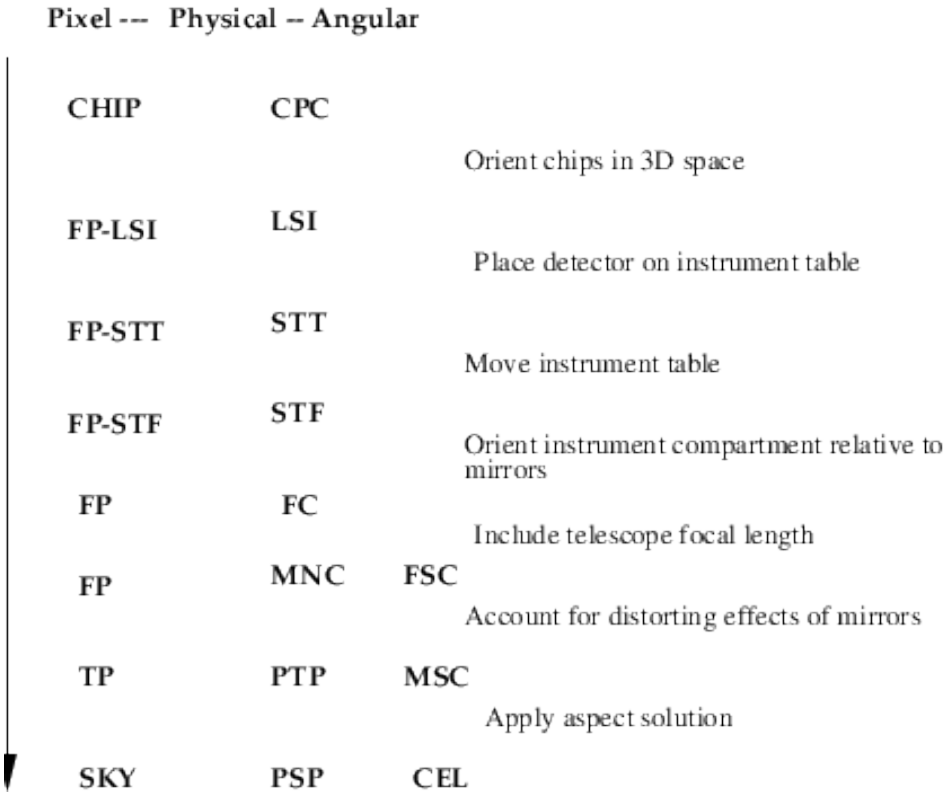

Figure 15: Coordinate systems used in data analysis, 1: Imaging data analysis.

detectors which do not include any tilted or out-of-plane chips (pre-AXAF missions), the calculation is much easier as you can just find the LSI coordinates of the ray when it hits the focal plane.

In our more complicated situtation, as before a general point on one of the detector planes is

$$\boldsymbol{r} = \boldsymbol{p_0} + X_{CPC}\boldsymbol{e}_X + Y_{CPC}\boldsymbol{e}_Y \tag{29}$$

where $\boldsymbol{p_0}$ is the origin of CPC coordinates, and $\boldsymbol{e}_X$ and $\boldsymbol{e}_Y$ are the unit vectors along the CPC axes, with $\boldsymbol{e}_Z$ as the unit normal to the plane.

The general ray is

$$\boldsymbol{r} = \boldsymbol{l_0} + \lambda \boldsymbol{l} \tag{30}$$

where $\boldsymbol{l_0}$ is an arbitrary point on the ray (the output of ray trace or else for approximate calculations, the mirror node), $\boldsymbol{l}$ is the ray direction, and λ labels positions along the ray. The intersection with the plane is then at

$$\boldsymbol{r} = \boldsymbol{l_0} + \frac{(\boldsymbol{p_0} - \boldsymbol{l_0}).\boldsymbol{e}_Z}{\boldsymbol{l}.\boldsymbol{e}_Z}\boldsymbol{l} \tag{31}$$

and we find CPC X and Y by taking the dot product with the CPC unit vectors,

$$X_{CPC} = \boldsymbol{r}.\boldsymbol{e}_X, \quad Y_{CPC} = \boldsymbol{r}.\boldsymbol{e}_Y \tag{32}$$

3.4.3 Chip coordinates

We can then recover chip coordinates and telemetry coordinates using the equations from previous sections.

$$\begin{aligned} CHIPX &= X_{CPC}/\Delta_p + 0.5 \\ CHIPY &= Y_{CPC}/\Delta_p + 0.5 \end{aligned} \tag{33}$$

3.5 Summary of imaging coordinate systems

Some of the physical coordinate systems, representing either a 3-D position or a 2-D angular position, has a corresponding 2-D pixel coordinate system used for display purposes and for practical storage in cases where the third dimension is redundant.

In the following table, I give each physical system with the corresponding pixel plane systems where applicable.

Physical System	Name	Pixel System	Params	Description
CPC	Chip Physical	CHIP	Inst. ID, Chip ID	Single chip
LSI	Local SI	-	Inst. ID	Focal plane, offset uncorrected
STT	SI Translation Table	-	Pixel size	Focal plane, offset uncorrected
STF	SI Translation Frame	-	Pixel size	Focal plane, alignment uncorrected
FC	Focus Coordinates	-	Pixel size	Focal plane
MNC	Mirror Nodal	DET	Pixel size	Focal plane
FSC	Focal Surface		Pixel size	Focal plane
MSC	Mirror Spherical	DET	Pixel size	Tangent plane
CEL	Celestial	SKY	Pixel size	Aspect applied
PTP	Physical Tangent Plane		Pixel size	Tangent Plane 3D

3.6 Data Analysis 3: Full treatment with misalignments

The discussion of transforming STF to MNC coordinates above is incomplete. For the full treatment, we consider misalignment of the telescope and optical bench, and include a background spacecraft (or lab) coordinate frame. For instance, at Chandra calibration the background coordinate frame is the XRCF system.

We define the following new frames:

- SC, the spacecraft frame (the XRCF frame plays this role in calibration)

- DFC, the frame along whose axes the STF frame (the science instrument module) is mechanically displaced and rotated. The origin of the DFC is the optical axis in the focal plane.
- MFC, the mirror fiducial coordinate system along whose axes the mirror is commanded to move.

Then a point in STF coordinates can be converted to spacecraft coords by

$$P(DFC) = O_{STF}(DFC) + R(DFC, STF)P(STF)$$

and

$$P(SC) = O_{DFC}(SC) + R(SC, DFC)P(DFC)$$

Here $O_{DFC}(SC)$ is the position in spacecraft coords of the home position of the SIM assembly $O_{STF}(DFC)$ is the displacement of the SIM assembly relative to this home position, and R(DFC,STF) is the rotation of the assembly relative to its home orientation. R(SC,DFC) gives the misalignment of the spacecraft and DFC frames. We further allow an independent motion of the mirror relative to the spacecraft frame.

$$P(SC) = O_{MFC}(SC) + R(SC, MFC)P(MFC)$$

and

$$P(MFC) = O_{MNC}(MFC) + R(MFC, MNC)P(MNC)$$

Here $O_{MFC}(SC)$ is the position of the center of rotation of the telescope in spacecraft coordinates, R(SC,MFC) give the misalignment of the zero of pitch and yaw relative to the SC system, and $R(MFC, MNC)$ gives the orientation of the mirrors. $O_{MNC}(MFC)$ allows for a translation of the mirror node relative to the center of rotation.

For the specific case of Chandra we have:

Parameter	Name	Flight	XRCF
$O_{MNC}(MFC)$	Nodal offset of center of rotn.	Zero	Zero?
$O_{MFC}(SC)$	SC coords of center of rotn.	Node	Node
$O_{DFC}(SC)$	SC coords of fiducial point	OTA focus	FOA
$O_{STF}(DFC)$	SIM frame displacement	Best focus, boresight	FAM displacement
R(MFC,MNC)	Mirror pitch and yaw	Zero	HRMA pitch, yaw
R(SC,MFC)	Mirror misalignment	Zero?	Mirror alignment
R(DFC,STF)	SIM frame orientation	Zero	FAM rotation
R(SC,DFC)	SIM frame misaligment	Boresight	FAM misalignment

The FITS keywords STG_X,Y,Z give the SIM frame displacement, as distinct from SIM_X,Y,Z which give the SIM table position relative to the SIM frame.

3.7 Data Analysis Coordinate Systems - Gratings

We now consider objective transmission gratings placed between the mirrors and the detectors.

When we observe with the gratings, we get a dispersed spectrum with orders +1, -1, +2, -2, ... and a zero-order undispersed image. The undispersed (zero-order) photons do not interact with the gratings and we can deal with them using the same analysis as for imaging detectors. To analyse a dispersed photon, however, we must know the location of the zero-order image as well as that of the dispersed photon. For instance, spacecraft roll aspect must be applied to the zero-order position, not the dispersed position.

The location of the zero order photon must be calculated relative to the Grating Node rather than the Mirror Node. The Grating Node is on the optical axis at a distance R from the focus, where R is the diameter of the Rowland Circle.

Each grating is defined by a grating node position and a grating pole vector which defines the cross-dispersion direction.

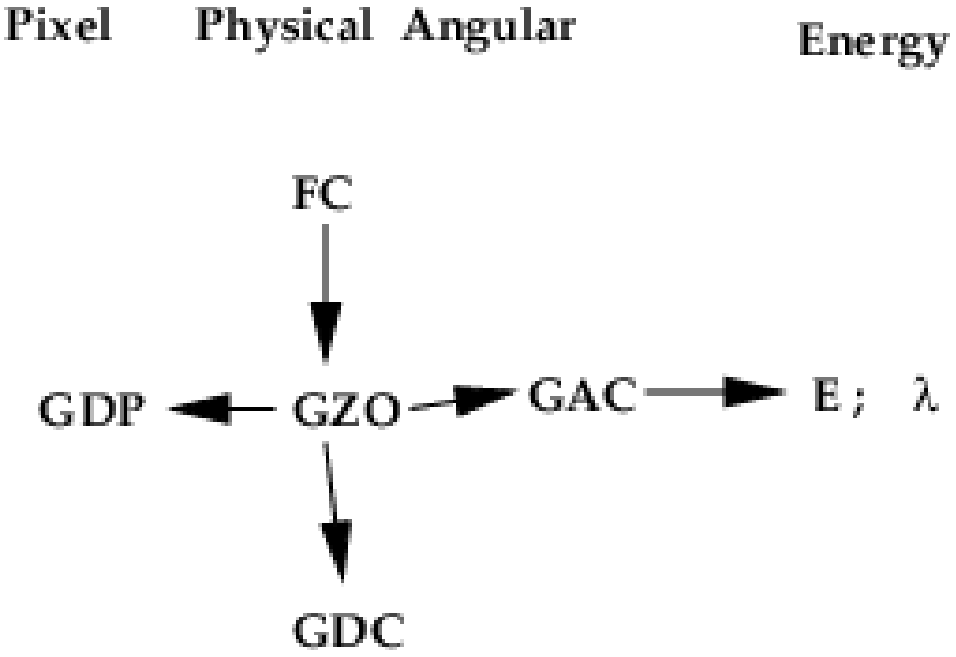

Figure 16: Coordinate systems used in data analysis, 2: Grating data analysis.

3.7.1 Grating Zero Order Coordinates (GZO)

Now we pick a source, with zero order position $\boldsymbol{ZO}$. and let the vector from the grating node to the source zero order be $\boldsymbol{S}$. Then define

$$\begin{aligned} \boldsymbol{e}_{X_{ZO}} &= -\boldsymbol{S}/|\boldsymbol{S}| \\ \boldsymbol{e}_{Y_{ZO}} &= \boldsymbol{d_0} \wedge \boldsymbol{e}_{X_{ZO}}/|\boldsymbol{d_0} \wedge \boldsymbol{e}_{X_{ZO}}| \\ \boldsymbol{e}_{Z_{ZO}} &= \boldsymbol{e}_{X_{ZO}} \wedge \boldsymbol{e}_{Y_{ZO}} \end{aligned} \tag{34}$$

where the Grating Pole (cross-dispersion unit vector) $\boldsymbol{d_0}$ is

$$\boldsymbol{d_0} = (0, -\sin\alpha_G, \cos\alpha_G) \tag{35}$$

in MNC coordinates, where α_G is the angle between the dispersion direction and the spacecraft Y axis.

This defines a cartesian orthonormal set, Grating Zero Order Coordinates, whose origin we choose to be at $\boldsymbol{G0}$. Diffracted photons travel in the X_{ZO}, Y_{ZO} plane, and the intersection of this plane with the detector surface defines the dispersion direction.

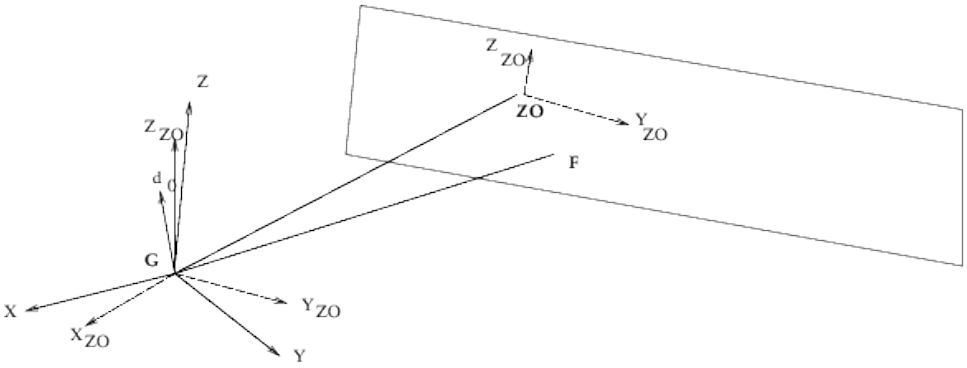

Figure 17: Grating Zero Order coordinates

The key step is calculating the GZO to FC transformation matrix. The columns of this matrix are simply the vectors $\boldsymbol{e}_{X_{Z0}}$ etc.

The GZO coordinates of the photon are then

$$P(GZO) = R(FC, GZO)(P(FC) - O_{GZO}(FC)) \tag{36}$$

where $O_{GZO}(LSI)$ are the FC coordinates of the grating node.

For an approximate treatment (which can be in error by several pixels), we can write the zero order coords as

$$ZO(FC) = (X, Y, Z) = (gX_o, gY_o, gZ_o) \tag{37}$$

where g is the distance from G0 to the focus. Then to first order

$$|S| = g(1 - X_o) \tag{38}$$

and

$$\begin{aligned} \boldsymbol{e}_{X_{ZO}} &= (1, -Y_o, -Z_o) \\ \boldsymbol{e}_{Y_{ZO}} &= ((Z_o \sin\alpha_G + Y_o \cos\alpha_G), \cos\alpha_G, \sin\alpha_G) \\ \boldsymbol{e}_{Z_{ZO}} &= (-Y_o \sin\alpha_G + Z_o \cos\alpha_G, -\sin\alpha_G, \cos\alpha_G) \end{aligned} \tag{39}$$

so that a point with FC coords (x, y, z) will have GZO coords

$$P(GZO) = (x - g, (y - Y)\cos\alpha_G + (z - Z)\sin\alpha_G, (z - Z)\cos\alpha_G - (y - Y)\sin\alpha_G) \tag{40}$$

3.7.2 Grating Angular Coordinates (GAC)

Grating Angular Coordinates (GAC) are the most important system for grating analysis. The GAC system (θ_r, θ_d) is a 2D angular system giving longitude and latitude with respect to GZO coordinates. The longitude coordinate, θ_r, is the **dispersion angle** and the latitude coordinate, θ_d, is the **cross-dispersion** angle. They are defined as

$$\begin{aligned} \theta_r &= \tan^{-1}\left(\tfrac{-Y_{ZO}}{X_{ZO}}\right) && \sim -Y_{ZO}/X_{ZO} \\ \theta_d &= \tan^{-1}\left(\tfrac{+Z_{ZO}}{\sqrt{X_{ZO}^2 + Y_{ZO}^2}}\right) && \sim +Z_{ZO}/X_{ZO} \end{aligned} \tag{41}$$

3.7.3 Grating Diffraction Coordinates (GDC)

The Grating Diffraction Coordinate system (r_{TG}, d_{TG}) gives the distance in mm along the dispersion direction and in the cross-dispersion direction. This is just related to the GAC coordinates by a simple scaling

$$\begin{aligned} r_{TG} &= X_R \theta_r \\ d_{TG} &= X_R \tan\theta_d \end{aligned} \tag{42}$$

Here X_R is the length from the grating node to the focus, which is approximately equal to the length $|\boldsymbol{S}|$.

3.7.4 Grating Diffraction Plane Pixel Coordinates (GDP)

The Grating Diffraction Plane Pixel Coordinates GDX, GDY are defined by

$$\begin{aligned} GDX &= GDX0 - \Delta_{gs}^{-1}(Y_{ZO}/X_{ZO}) \\ GDY &= GDY0 + \Delta_{gs}^{-1}(Z_{ZO}/X_{ZO}) \end{aligned} \tag{43}$$

analogously to the Focal Plane Pixel Coordinates.

They are related to the physical Grating Diffraction Coordinates by

$$\begin{aligned} GDX &= GDX0 + \Delta_{gs}^{-1}\tan(r_{TG}/X_R) \\ GDY &= GDY0 + \Delta_{gs}^{-1}(d_{TG}/X_R)\cos(r_{TG}/X_R) \end{aligned} \tag{44}$$

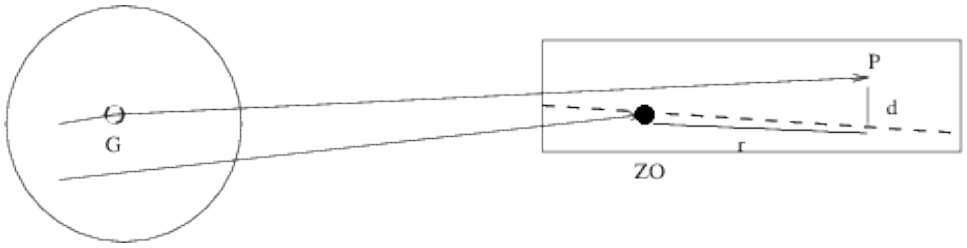

Figure 18: Grating Diffraction coordinates

3.7.5 Dispersion relation

The wavelength of the diffracted photon is

$$\lambda = P \sin \theta_R / m \tag{45}$$

where P is the average grating period and m is the diffraction order. So

$$\lambda \sim (P/m)(GDX - GDX0)\Delta_{gs} \tag{46}$$

4 Chandra specifics

4.1 ACIS

4.1.1 Overview

The ACIS instrument has 10 CCD chips. In the event list data, each is identified by an integer from 0 to 9. Four of the chips, the imaging set, are arranged in a rough square (but individually tilted). Six are the spectroscopic array, arranged in a line.

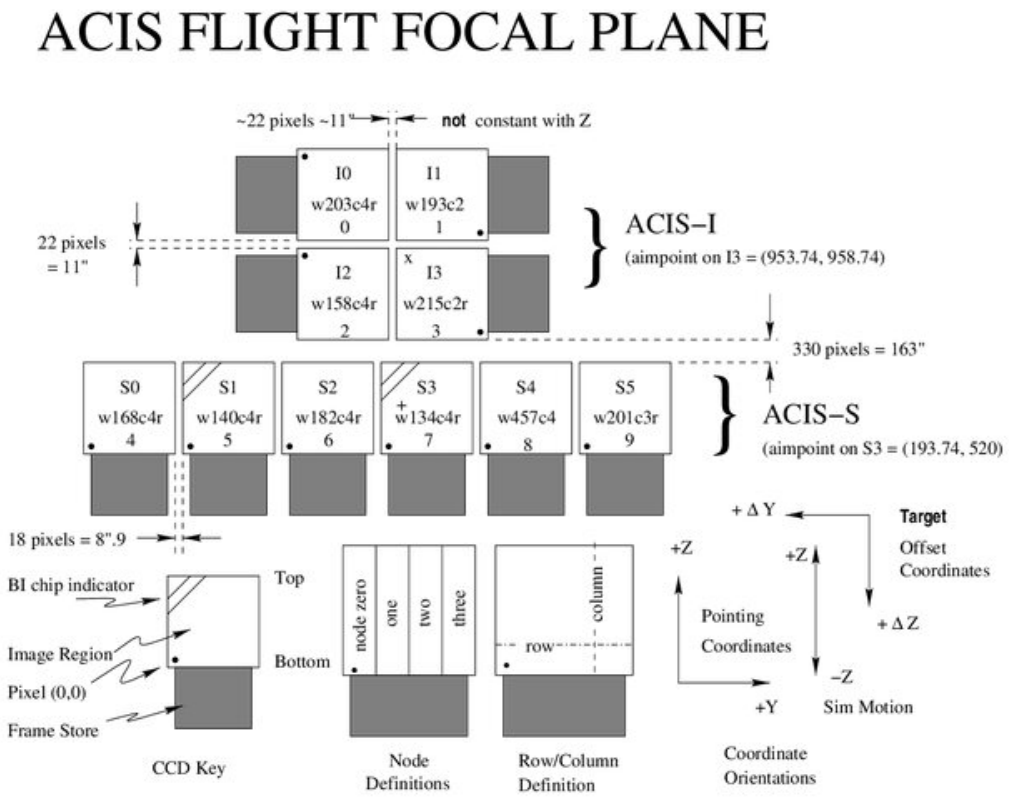

Figure 19: ACIS layout (Source: POG Chapter 6)

Chip Name	CHIP ID
ACIS-I0	0
ACIS-I1	1
ACIS-I2	2
ACIS-I3	3
ACIS-S0	4
ACIS-S1	5
ACIS-S2	6
ACIS-S3	7
ACIS-S4	8
ACIS-S5	9

The CHIP ID is also called CCD ID for consistency with ASCA.

4.1.2 ACIS Instrumental details - readout coordinates

ACIS Readout Coordinates are used internally by ACIS and may be seen in subassembly cal (SAC) data, but in flight the Chip coordinates are calculated on board and telemetered directly. Users don't deal with the readout coordinates. They are discussed here for completeness.

The ACIS readout coordinate system was explained in a 1995 draft memo from J Woo. This memo defines two coordinate systems, the "pixel coordinate system of the readout file array, f(x,y)", which I will call the **ACIS Readout Coordinates** $(XREAD, YREAD)$ and the "pixel coordinate system of the active detector image array p(x,y)", which I will call **ACIS Chip Coordinates**, $(XCHIP, YCHIP)$ (these are the ones that run from 1 to 1024).

The two systems, readout and Chip, are related by

$$YCHIP = \begin{cases} YREAD & 1 \leq YREAD \leq 1026 \\ \text{Overclock} & 1027 \leq YREAD \leq 1030 \end{cases} \quad (47)$$

$$XCHIP = \begin{cases} \text{Underclock} & 1 \le XREAD \le 4 & \\ XREAD - 4 & 5 \le XREAD \le 260 & \text{(Node A)} \\ \text{Overclock} & 261 \le XREAD \le 337 & \\ \text{Undefined Parallel Transfer} & 338 \le XREAD \le 340 & \\ \text{Underclock} & 341 \le XREAD \le 344 & \\ 857 - XREAD & 345 \le XREAD \le 600 & \text{(Node B} \\ \text{Overclock} & 601 \le XREAD \le 677 & \\ \text{Undefined Parallel Transfer} & 678 \le XREAD \le 680 & \\ \text{Underclock} & 681 \le XREAD \le 684 & \\ XREAD - 172 & 685 \le XREAD \le 940 & \text{(Node C)} \\ \text{Overclock} & 941 \le XREAD \le 1017 & \\ \text{Undefined Parallel Transfer} & 1018 \le XREAD \le 1020 & \\ \text{Underclock} & 1021 \le XREAD \le 1024 & \\ 2049 - XREAD & 1025 \le XREAD \le 1280 & \text{(Node D)} \\ \text{Overclock} & 1281 \le XREAD \le 1357 & \\ \text{Undefined Parallel Transfer} & 1358 \le XREAD \le 1360 & \end{cases} \tag{48}$$

The inverse transformation is

$$\begin{aligned} YREAD &= YCHIP \\ XREAD &= \begin{cases} XCHIP + 4 & 1 \le XCHIP \le 256 & \text{(A)} \\ 857 - XCHIP & 257 \le XCHIP \le 512 & \text{(B)} \\ XCHIP + 172 & 513 \le XCHIP \le 768 & \text{(C)} \\ 2049 - XCHIP & 769 \le XCHIP \le 1024 & \text{(D)} \end{cases} \end{aligned} \tag{49}$$

4.1.3 3-D chip locations: CPC to LSI transformation parameters

In the following tables we list the CPC and LSI coordinates of each corner of each chip. We give coordinates for each of the ACIS chips in both the ACIS-I and ACIS-S LSI systems, since we may take data from ACIS-S chips while ACIS-I is in the focus or vice versa. The systems are simply offset by 46.88mm in the Z_{LSI} direction. The ACIS data was originally from ACIS-SOP-01 but has been slightly updated post launch.

The HRC data is deduced from information provided by M. Juda.

The LSI system is used to record the fiducial light positions (which are needed for the aspect solution) in the pcad/align calibration files).

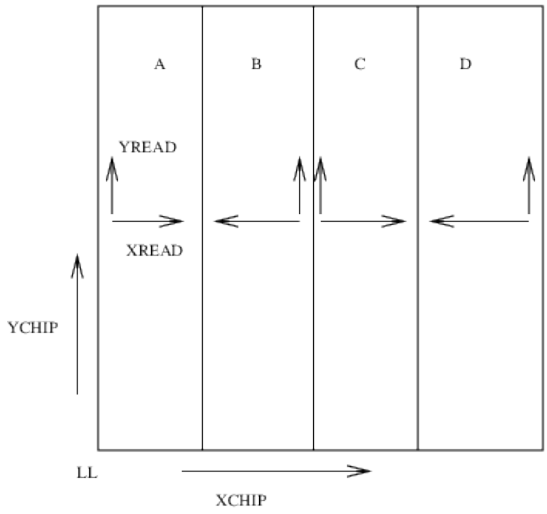

Figure 20: ACIS readout nodes

Table 3: ACIS Chip corner locations in ACIS-I LSI coordinates

Chip	Corner	CPC coords	ACIS-I LSI coords
I0	LL	(0.0, 0.0, 0.0)	(2.361, -26.483, 23.076)
	LR	(24.58, 0.0, 0.0)	(1.130, -26.545, -1.456)
	UR	(24.58, 24.58, 0.0)	(-0.100, -2.013, -1.456)
	UL	(0.0, 24.58, 0.0)	(1.130, -1.951, 23.076)
I1	LL	(0.0, 0.0, 0.0)	(1.130, 23.078, -1.446)
	LR	(24.58, 0.0, 0.0)	(2.360, 23.016, 23.086)
	UR	(24.58, 24.58, 0.0)	(1.130, -1.515, 23.086)
	UL	(0.0, 24.58, 0.0)	(-0.100, -1.453, -1.446)
I2	LL	(0.0, 0.0, 0.0)	(1.130, -26.550, -1.992)
	LR	(24.58, 0.0, 0.0)	(2.361, -26.488, -26.525)
	UR	(24.58, 24.58, 0.0)	(1.130, -1.956, -26.525)
	UL	(0.0, 24.58, 0.0)	(-0.100, -2.018, -1.992)
I3	LL	(0.0, 0.0, 0.0)	(2.361, 23.011, -26.530)
	LR	(24.58, 0.0, 0.0)	(1.131, 23.073, -1.997)
	UR	(24.58, 24.58, 0.0)	(-0.100, -1.458, -1.997)
	UL	(0.0, 24.58, 0.0)	(1.130, -1.520, -26.530)
S0	LL	(0.0, 0.0, 0.0)	(0.744, -81.14, -59.208)

	LR	(24.58, 0.0, 0.0)	(0.353, -56.555, -59.196)
	UR	(24.58, 24.58, 0.0)	(0.353, -56.567, -34.633)
	UL	(0.0, 24.58, 0.0)	(0.744, -81.126, -34.645)
S1	LL	(0.0, 0.0, 0.0)	(0.348, -56.090, -59.196)
	LR	(24.58, 0.0, 0.0)	(0.099, -31.530, -59.176)
	UR	(24.58, 24.58, 0.0)	(0.099, -31.550, -34.613)
	UL	(0.0, 24.58, 0.0)	(0.348, -56.110, -34.634)
S2	LL	(0.0, 0.0, 0.0)	(0.096, -31.076, -59.183)
	LR	(24.58, 0.0, 0.0)	(-0.011, -6.514, -59.164)
	UR	(24.58, 24.58, 0.0)	(-0.011, -6.534, -34.601)
	UL	(0.0, 24.58, 0.0)	(0.096, -31.096, -34.621)
S3	LL	(0.0, 0.0, 0.0)	(-0.011, -6.026, -59.166)
	LR	(24.58, 0.0, 0.0)	(0.024, 18.535, -59.153)
	UR	(24.58, 24.58, 0.0)	(0.024, 18.522, -34.591)
	UL	(0.0, 24.58, 0.0)	(-0.011, -6.039, -34.604)
S4	LL	(0.0, 0.0, 0.0)	(0.026, 18.963, -59.153)
	LR	(24.58, 0.0, 0.0)	(0.208, 43.524, -59.141)
	UR	(24.58, 24.58, 0.0)	(0.208, 43.512, -34.579)
	UL	(0.0, 24.58, 0.0)	(0.026, 18.951, -34.591)
S5	LL	(0.0, 0.0, 0.0)	(0.208, 43.958, -59.138)
	LR	(24.58, 0.0, 0.0)	(0.528, 68.518, -59.128)
	UR	(24.58, 24.58, 0.0)	(0.528, 68.508, -34.566)
	UL	(0.0, 24.58, 0.0)	(0.208, 43.948, -34.575)

4.1.4 Special case: ACIS subarray mode

Subarray mode (originally called Fast Window mode) is used for some ACIS observations. The coordinates within the window are corrected to ACIS chip coordinates in the pipeline and are not seen by users.

In window mode, we get an initial set of Window Chip Coordinates WX, WY which run from 1 to 1024 and 1 to WSIZE. WSIZE is a configurable number that is different for different observations. There is no way to uniquely know from the telemetry what the true ACIS chip coordinates of the photon were - you get an uncertainty modulo WSIZE. However, to calculate best guess ACIS chip coordinates we can assume that the photon is associated with a known incident source location, resolving the uncertainties.

For non grating data, calculate the predicted ACIS Chip coordinates for the incident radiation, say (CX0, CY0). At XRCF, this will involve the forward calculation including the STF coordinates of the FAM. Then set

```
CY1 = (CY0 / WSIZE ) * WSIZE
```

using integer arithmetic. Then

$$CHIPX = WX \tag{50}$$

and

$$CHIPY = WY + CY1 \tag{51}$$

4.1.5 Obsolete case: 2-D detector coordinates, TDET parameters

The TDET tiled detector coordinates are implemented for AXAF with the following specific systems, each of which specifies a TDET system in terms of the CHIP coordinates.

Table 4: Tiled Detector Plane systems

System	Size	X Center, Y Center	Use
AXAF-ACIS-2.2	8192 x 8192	(4096.5, 4096.5)	Standard

Table 5: Parameters of Tiled Detector Coordinate definitions

Tiled System	Chip	θ_i	Δ_i	$X0_i$	$Y0_i$	H_i
AXAF-ACIS-2.2	ACIS-I0	90	1	3061.0	5131.0	1
AXAF-ACIS-2.2	ACIS-I1	270	1	5131.0	4107.0	1
AXAF-ACIS-2.2	ACIS-I2	90	1	3061.0	4085.0	1
AXAF-ACIS-2.2	ACIS-I3	270	1	5131.0	3061.0	1
AXAF-ACIS-2.2	ACIS-S0	0	1	791.0	1702.0	1
AXAF-ACIS-2.2	ACIS-S1	0	1	1833.0	1702.0	1
AXAF-ACIS-2.2	ACIS-S2	0	1	2875.0	1702.0	1
AXAF-ACIS-2.2	ACIS-S3	0	1	3917.0	1702.0	1
AXAF-ACIS-2.2	ACIS-S4	0	1	4959.0	1702.0	1
AXAF-ACIS-2.2	ACIS-S5	0	1	6001.0	1702.0	1

4.2 HRC

4.2.1 Overview

The HRC instrument has two detectors, the HRC-S and the HRC-I. The HRC-I has a single 'chip' or segment/microchannel plate pair (CHIP ID = 0, name HRC-I) while the HRC-S has three (CHIP ID = 1,2,3; name HRC-S1,S2,S3; HRC team segment designation +1, 0, -1). We define an HRC-I chip plane which is 16384 pixels square; (not all of these pixels correspond to actual readable values); the HRC-S chips are 4096 x 16456 pixels The pixel size is 0.0064294 mm.

Name	ID	CHIP size (pix)	Pixel size (μ)	CHIP size (mm)
HRC-I	0	16384 x 16384	6.429 x 6.429	105.333 x 105.333
HRC-S1	1	4096 x 16456	6.250 x 6.429	25.600 x 105.802
HRC-S2	2	4096 x 16456	6.250 x 6.429	25.600 x 105.802
HRC-S3	3	4096 x 16456	6.250 x 6.429	25.600 x 105.802

4.2.2 HRC physical layout and taps

Each HRC sub-instrument contains a series of electrical 'taps' on each axis of the wire grid, which define a continuous spatial system. The electrical axes are labelled u and v, and we will say there are N_u and N_v taps on each axis, numbered starting at 0. In the internal HRC-S electronics the three MCPs have individually numbered taps but these are combined before we see it in the telemetry. The coarse tap positions are modified by a fine position which runs from -0.5 to +0.5. Then we can define an **HRC Tap Coordinate System** which runs from $u = -0.5$ to $u = N_u - 0.5$, and $v = -0.5$ to $N_v - 0.5$.

4.2.3 AMPSF parameter

The AMPSF parameter $\hat{A}$ is used in the degapping correction and the tap ring correction. Its value depends on the event's PHA value p and the 'scaled sum amps', $s = \frac{1}{2}S/g$ where S is the sum of the three amp values for both axes (so, sum of six values in all) and g is a gain parameter equal to 52.90.

We define boundary PHA values p_b as follows:

$$\begin{aligned} p_b(1) &= p_{12} - w_{12} \\ p_b(2) &= p_{12} + w_{12} \\ p_b(3) &= p_{23} - w_{23} \\ p_b(4) &= p_{23} + w_{23} \end{aligned}$$

where the coefficients are read from the AMP SF COR calibration file. The values for a range switch level between 90 and 125 are:

p_{12}	w_{12}	p_{23}	w_{12}
70.5	5.0	137.50	5.0

which result in boundaries

$p_b(1)$	$p_b(2)$	$p_b(3)$	$p_b(4)$
65.5	75.5	132.50	142.5

We also define the test function

$$f(p, s, r) = |p - rs| - |p - 2rs|$$

Then

$$\hat{A} = \begin{cases} 1 & (p < p_b(1)) \\ 1 & (p_b(1) \le p < p_b(2)) \quad \text{and} \quad f(p, s, 1) > 0 \\ 2 & (p_b(1) \le p < p_b(2)) \quad \text{and} \quad f(p, s, 1) \le 0 \\ 2 & (p_b(2) \le p < p_b(3)) \\ 2 & (p_b(3) \le p < p_b(4)) \quad \text{and} \quad f(p, s, 2) > 0 \\ 3 & (p_b(3) \le p < p_b(4)) \quad \text{and} \quad f(p, s, 2) \le 0 \\ 3 & (p \ge p_b(4)) \end{cases}$$

4.2.4 Tap ring correction

HRC event positions are affected by a correction to the third amplifier value, using parameters frome the TAPRINGTEST calibration file (tabulated below) and the amplifier values a_{ij}, where i = 1 or 2 for U and V, and j runs from 1 to 3.

Parameter	U axis	V axis
A	-24	-40
B	-690	-655
C	0.279	
D	530	655
β	6.7	0.0
γ	1.75	1
T_1 (THRESH)	0	
T_0 (OFFSET)	0	

We define

$$\tau = T_0 + a_{i1} T_1$$

- note that this parameter is zero for the calibration currently used and listed above.

We make the tap correction separately for each of the two axes U and V (i = 1, 2). The correction is made for axis i if

- The AMPSF parameter $\hat{A} = 3$;
- All the a_{ij} are positive, j = 1 to 3;
- $a_{i1} > a_{i3}$; and
- $a_{i1} > \tau$.

The correction, when made, is

$$\Delta a_{i3} = -\left(\frac{a_{i1}+B}{A}\right)\sin(2\pi f)$$

where

$$f = \left[\frac{a_{i1} - \beta\left(\left(\frac{a_{i2}}{a_{i1}}\right)^{\gamma} - 1\right)}{Ca_{i2}+D}\right]$$

The the new value of the third amplifier is

$$a_{i3}(\text{new}) = a_{i3}(\text{old}) + \Delta a_{i3}$$

4.2.5 The degap problem - coarse and fine coordinates

The instrument electronics records four numbers per axis for each event: the 'center tap' (usually the tap with the maximum voltage), and the voltages of that tap and the one on either side. These numbers, which are the values which get coded into flight telemetry, we will refer to as **HRC telemetry coordinates** $(\mathbf{u}_{ht}, \mathbf{v}_{ht})$. The four integer components of $\mathbf{u}_{ht}$ are

$$\mathbf{u}_{ht} = \begin{cases} u_0 & \text{Max tap, 0 to } N_u - 1 \text{ ('coarse position')} \\ \text{ADC1} & \text{Voltage of } u_{\text{coarse}} - 1 \\ \text{ADC2} & \text{Voltage of } u_{\text{coarse}} \\ \text{ADC3} & \text{Voltage of } u_{\text{coarse}} + 1 \end{cases} \tag{52}$$

and similarly for $\mathbf{v}_{ht}$). From the telemetry coordinates we can calculate an intermediate quantity, the **fine position**

$$u_{\text{fine}} = \frac{\text{ADC3} - \text{ADC1}}{\text{ADC1} + \text{ADC2} + \text{ADC3}} \tag{53}$$

Note that

$$-0.5 \le u_{\text{fine}} \le +0.5 \tag{54}$$

We now split off the sign of this fine position correction to obtain the tap side

$$s_u = \begin{cases} +1 & (u_{\text{fine}} \ge 0) \\ -1 & (u_{\text{fine}} < 0) \end{cases} \tag{55}$$

and the fine position magnitude

$$\Delta u = |u_{\text{fine}}| \tag{56}$$

From these we calculate the linear HRC Tap Coordinates

$$\begin{aligned} u &= u_0 + s_u C_{u1}(u_0, s_v)\Delta u - s_u C_{u2}(u_0, s)\Delta u^2 \\ v &= v_0 + s_v C_{v1}(v_0, s_v)\Delta v - s_v C_{v2}(v_0, s)\Delta v^2 \end{aligned} \tag{57}$$

The C factors are called the **degapping parameters**; for HRC they have different values for each tap and tap side. Earlier detectors (Einstein and Rosat HRI) assumed C factors which were independent of coarse position.

4.2.6 The degap problem - raw coordinates

The simplest choice of the degapping parameters is to take

$$\begin{aligned} C_{u1} &= C_{v1} = 1 \\ C_{u2} &= C_{v2} = 0, \end{aligned} \tag{58}$$

giving us **HRC raw tap coordinates**,

$$\begin{aligned} u_{raw} &= (u_{\text{coarse}} + u_{\text{fine}}) \\ v_{raw} &= (v_{\text{coarse}} + v_{\text{fine}}) \end{aligned} \tag{59}$$

We define HRC Raw pixel coordinates by

$$\begin{aligned} RAWU &= (u_{raw} + 0.5) * \Delta_t \\ RAWV &= (v_{raw} + 0.5) * \Delta_t, \end{aligned} \tag{60}$$

integer pixel numbers which start with pixel 0 (for a tap value of -0.5). Here the tap size Δ_t is 256 pixels.

These coordinates do not provide a continuous system over the detector, and an HRC image plotted in raw coordinates contains 'gaps'.

4.2.7 HRC Telemetry Coordinates

The HRC Telemetry Pixel Number System applies the degap correction to the raw coordinates to give the linearized 'telemetry' or 'degapped' coordinates

$$TELU = RAWU + \Delta_u(A, RAWU) \tag{61}$$

$$TELV = RAWV + \Delta_v(A, RAWV) \tag{62}$$

$$\tag{63}$$

integer pixel numbers which start with pixel 0 (for a tap value of -0.5).

The Δ_u and Δ_v functions are tabulated The 'degap map' calibrations are in the CALDB in the hrc/gaplookup directory. There are three sets of calibrations, one for each value of the AMPSF parameter A of the event.

The figure shows an segment from the HRC-S V-axis degap map. The sawtooth pattern has discontinuities at the tap boundaries.

4.2.8 HRC Chip Coordinates

For compatibility with other data archives, instead of these telemetry coordinates we divide up the HRC into individual chips to get HRC Chip Coordinates

For each instrument segment,

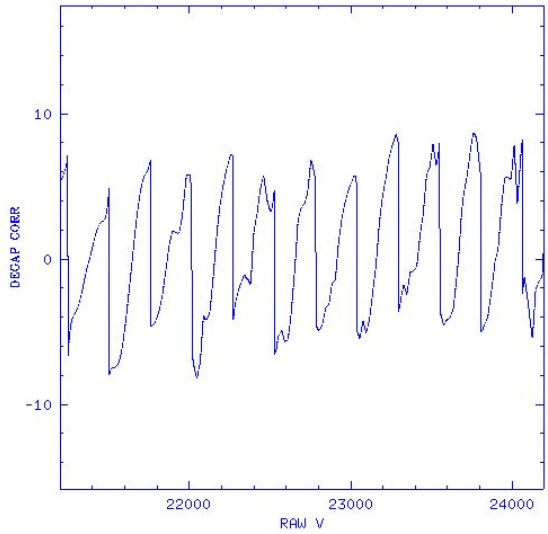

Figure 21: Region of HRC-S V-axis degap map, showing Δ_v(RAWV) in pixels vs RAWV

$$CHIPX = TELU + NOM\_OFF\_X + HRC\_OFF\_X \quad (64)$$
$$CHIPY = TELV + NOM\_OFF\_Y + HRC\_OFF\_Y \quad (65)$$
$$(66)$$

The following parameters are stored in the degap lookup file. The idea of using the NOM_OFF values is just to keep the variable adjustments small in magnitude. There is a degeneracy between the degap solution and the offsets which must keep constant the astrometry. (If the degap solution changes, the mean TEL coordinates of all the events may change, and to keep the same chip-to-sky WCS, we soak up the change in the offsets). In an ideal world the degap solution should be adjusted so that OFF_X (and perhaps OFF_Y) values are all zero.

	NOM OFF X	NOM OFF Y	HRC OFF X	HRC OFF Y
HRC-I	0.0	0.0	1.0	1.0
HRC-S1	0.0	0.0	1.0	20.2
HRC-S2	0.0	-16384.0	1.0	-75.9
HRC-S3	0.0	-32768.0	-3.0	-165.3

It returns us to a system in which the coordinates are numbered separately for each chip.

Table 7: HRC-S1 TELV, v and CHIPY

TELV	Coarse v, Fine v	CHIPY

0	0, -0.5	-255
16640	64, +0.5	16384

In this system, 1 pixel = 0.0064294 mm = 0.13 arcsec. The size of one tap is 1.646mm. Now this coordinate system actually covers a larger area than the true possible coordinates. For instance, v taps 0 and 1 for HRC-S1 are missing, so the lowest possible v coordinate in the telemetry for HRC-S is 1.5 (corresponding to tap 2 with fine position -0.5) but even this does not correspond to a valid detected event position. Nevertheless, we will define our logical coordinate system to cover the range of v coordinates starting at CHIPX, CHIPY = 0.5 (lower left corner of first pixel) which corresponds to HRC-S u, v = (-0.5, +0.5).

The center of HRC-S2 is then at $(u, v) = (7.5, 95.5)$ and the gaps between the MCPs are at v values of 62.96 to 64.12 and 124.88 to 126.04. In earlier work I arbitrarily set the chip boundaries at 63.0 and 126.0 so that each chip has a length of 63.0 taps, but on recommendation from M. Juda I have adjusted the chip sizes so that the true chip gaps fall on the logical chip boundaries.

Table 8: HRC electronically meaningful coordinate ranges

Chip	v_0	u	v	CHIPX	CHIPY	TELU	TELV
HRC-I	-0.5	0.0 to 63.0	0.0 to 63.0	0.5 to 16128.5	0.5 to 16128.5		
HRC-S1	0.5	0.0 to 15.0	1.5 to 64.5	128.5 to 3968.5	256.5 to 16384.5		
HRC-S2	64.5	0.0 to 15.0	64.5 to 126.5	128.5 to 3968.5	0.5 to 15872.5		
HRC-S3	126.5	0.0 to 15.0	126.5 to 190.5	128.5 to 3968.5	0.5 to 16384.5		

Now let's look at the boundaries on HRC-S and HRC-I more closely. We keep extra figures for self-consistency only assuming a tap scale of 1.6460 exactly, and measure positions starting at the physical position corresponding to chip pixel position 0.5 (bearing in mind this may be outside of the wire grid).

I used the following information on the HRC-S:

```
Tap size is 1.646 mm (M. Juda)
16384 pixels = 105.344 mm: logical chip size = tap size 1.646 mm x 64 taps
MCP physical size 100.000 mm x 27.000 mm from 'TOP MCP COORDINATES' drawing
Total logical length is 3 x 105.344 mm
Total physical length is 3 x 100.000 mm + 2 x gap size = 1.905 mm.
S2 Center is center of both total logical and total physical length.
Coating extends 94.5mm on outer MCPs and 16mm wide (M. Juda)

Post XRCF revision 1: (M Juda Oct 97)
S1 TELU range from 600 to 3496, TELV from 1190 to 16250 with
CsI limit at 1613.
S2 TELU from 600 to 3488, TELV from 16990 to 32261
S3 TELU from 600 to 3504, TELV from 32925 to 48110 with CsI
limit at 47650.

The coating strip is at TELU = 2660 (S1), 2670 (S2), 2670 (S3)
with the 'T' strip at TELV from 22780 to 27670.

More accurate post XRCF data: MCP edges at TELV = 16428, 17012, 32244, 32932.
```

This information leads to the following MCP layout :

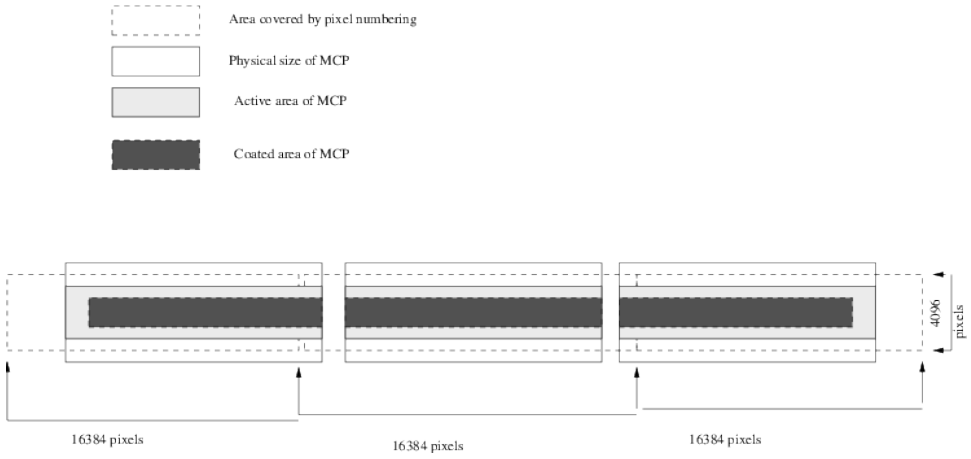

Figure 22: Relationship of HRC-S pixels to the physical instrument.

Table 9: HRC-S boundaries (Revised Jan 99)

Boundary	TELV	Tap v	Pos mm	Seg No.	Y_{CPC} mm	CHIPY pix
S1 Logical Left Edge	-12		0.000	1	0.000	0.5
S1 TELV = 0	0	-0.50	0.077	1	0.077	12.5
S1 Electronic L Edge	512	1.50	3.369	1	3.369	524.5
S1 MCP Left Edge	1196	4.17	7.767	1	7.767	1208.5
S1 Active Left Edge	1664	6.00	10.776	1	10.776	1676.5
S1 Active Right Edge	16404	63.58	104.545	1	105.545	16416.5
S1 MCP Right Edge	16444	63.73	105.802	1	105.802	16456.5
S1 Logical Right Edge	16444	63.73	105.802	1	105.802	16456.5
Gap left edge	16444	63.73	105.802	1	105.802	16456.5
Gap right edge	16459.9	63.80	105.802	1	105.802	16456.5
S2 Logical Left Edge	16460	63.80	105.802	2	0.000	0.5
S2 MCP Left Edge	16900	65.51	108.631	2	2.829	440.5
S2 Active Left Edge	17060	66.14	109.660	2	3.858	600.5
S2 Center	24576	95.50	157.983	2	52.181	8116.5
S2 Aimpoint	25198	97.93	161.982	2	56.180	8738.5
S2 Active Right Edge	32165	125.14	206.776	2	100.974	15705.5
S2 MCP Right Edge	32250	125.48	207.322	2	101.520	15790.5
S2 Logical Right Edge	32916.0	128.08	211.604	2	105.802	16456.5
S3 Logical Left Edge	32916.0	128.08	211.604	3	0.000	0.5
Gap left edge	32916.4	128.08	211.604	3	0.000	0.5
Gap right edge	32930.0	128.13	211.604	3	0.000	0.5
S3 MCP Left Edge	32930	128.13	211.604	3	0.000	0.5
S3 Active Left Edge	32940	128.17	211.668	3	0.064	10.5
S3 Active Right Edge	47605	185.46	305.955	3	94.351	14675.5
S3 MCP Right Edge	48117	187.46	309.247	3	97.643	15187.5
S3 Electronic R Edge	48640	189.50	312.604	3	101.000	15710.5
S3 Logical Right Edge	49386	192.41	317.406	3	105.802	16456.5

Boundary	TELU	Tap u	X_{CPC} mm	CHIPX pix
MCP Edge		-1.620	-0.700	-286.2
TELU = 0	0	-0.500	0.000	0.5
Logical Edge		-0.500	0.000	0.5

Active edge	560		3.500	560.5
Coating Edge		1.843	3.748	600.0
Center	2048	7.500	12.800	2048.5
Strip Edge		9.930	16.688	2670.0
Coating Edge		13.172	21.875	3500.0
Active edge	3536		22.10	3536.5
Logical Edge		15.500	25.600	4096.5
MCP Edge		15.937	26.300	4208.5

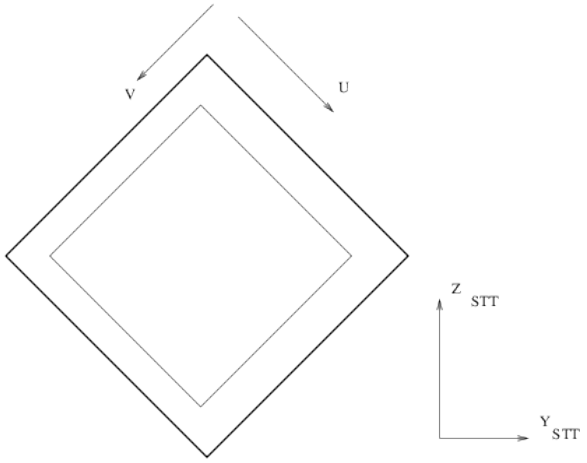

Figure 23: HRC-I pixel axes.

Table 10: HRC-I boundaries

Boundary	Tap u or v	X/Y$_{CPC}$ mm	CHIPX/Y pix
Logical Edge	-0.500	0.000	0.5
MCP Edge	1.123	2.672	416.1
Active Area	3.250	6.172	960.4
Coating Edge	4.161	7.672	1193.7
Center	31.500	52.672	8192.5
Coating Edge	58.839	97.672	15191.3
Active Area	59.750	99.172	15424.6
MCP Edge	61.877	102.672	15968.9
Logical Edge	63.500	105.344	16384.5

The CPC coordinates run from 0.0 to 26.33 (X$_{CPC}$ for HRC-S) and from 0.0 to 105.3 (Y$_{CPC}$ for HRC-S and both axes for HRC-I).

The active area of each microchannel plane is smaller, and the area coated with photocathode is smaller still. For HRC-I, the chip is 100 x 100 mm, with a 93 x 93 mm active area and a 90 x 90 mm coated area. For HRC-S, each chip is 100 x 27 mm, the active area is 100 x 20 mm, and the coated area is 94.5 x 16.0 mm. except for HRC-S2 where the coated area is 100 x 16 mm. Using these numbers, we derive the locations of the various areas in CPC (mm) and Chip (pixel) coordinates listed above.

4.2.9 3-D chip locations: CPC to LSI parameters

The corners of the logical chip planes are located in the LSI coordinate system as follows; these are calculated by placing the HRC-S origin (default aimpoint) at 4.0mm to +LSI Y of the overall detector center and using the chip sizes calculated above together with the designed S1 and S3 chip tilts in the X,Y plane. Note that S2 is no longer centered around the detector center, since its edges are determined by the measured gap locations.

Table 11: HRC chip (i.e. grid) corner locations in LSI coordinates

Chip	Corner	CPC coords	HRC-I,S LSI coords
HRC-I	LL	(0.000 , 0.000 , 0.000)	(0.000 , 0.000 , 74.481)
HRC-I	LR	(105.339 , 0.000 , 0.000)	(0.000 , 74.481 , 0.000)
HRC-I	UR	(105.339 , 105.339 , 0.000)	(0.000 , 0.000 , -74.481)
HRC-I	UL	(0.000 , 105.339 , 0.000)	(0.000 , -74.481 , 0.000)
HRC-S1	LL	(0.000 , 0.000 , 0.000)	(2.644 , 161.964 , -12.969)
HRC-S1	LR	(26.334 , 0.000 , 0.000)	(2.644 , 161.932 , 13.364)
HRC-S1	UR	(26.334 , 105.802 , 0.000)	(0.000 , 56.163 , 13.235)
HRC-S1	UL	(0.000 , 105.802 , 0.000)	(0.000 , 56.196 , -13.098)
HRC-S2	LL	(0.000 , 0.000 , 0.000)	(0.000 , 56.196 , -13.098)
HRC-S2	LR	(26.334 , 0.000 , 0.000)	(0.000 , 56.163 , 13.235)
HRC-S2	UR	(26.334 , 105.802 , 0.000)	(0.000 , -49.638 , 13.106)
HRC-S2	UL	(0.000 , 105.802 , 0.000)	(0.000 , -49.605 , -13.227)
HRC-S3	LL	(0.000 , 0.000 , 0.000)	(0.000 , -49.605 , -13.227)
HRC-S3	LR	(26.334 , 0.000 , 0.000)	(0.000 , -49.638 , 13.106)
HRC-S3	UR	(26.334 , 105.802 , 0.000)	(2.253 , -155.415 , 12.977)
HRC-S3	UL	(0.000 , 105.802 , 0.000)	(2.253 , -155.383 , -13.356)

4.2.10 Obsolete case: 2-D detector coordinates: TDET parameters

The ASC-TDET-1.0 tiled detector coordinates are implemented for AXAF with the following specific systems, each of which specifies a TDET system in terms of the CHIP coordinates.

Table 12: Tiled Detector Plane systems

System	Size	X Center, Y Center	Use
AXAF-HRC-2.3I	16384 x 16384	(8192.5, 8192.5)	Standard HRC-I
AXAF-HRC-2.6S	49368 x 4096	(24684.5, 2048.5)	Revised HRC-S

Table 13: Parameters of Tiled Detector Coordinate definitions

Tiled System	Chip	θ_i	Δ_i	$X0_i$	$Y0_i$	H_i
AXAF-HRC-2.3I	HRC-I	90	1	0.0	0.0	-1
AXAF-HRC-2.6S	HRC-S1	270	1	49368.0	0.0	1
AXAF-HRC-2.6S	HRC-S2	270	1	32912.0	0.0	1
AXAF-HRC-2.6S	HRC-S3	270	1	16456.0	0.0	1

4.3 The SIM

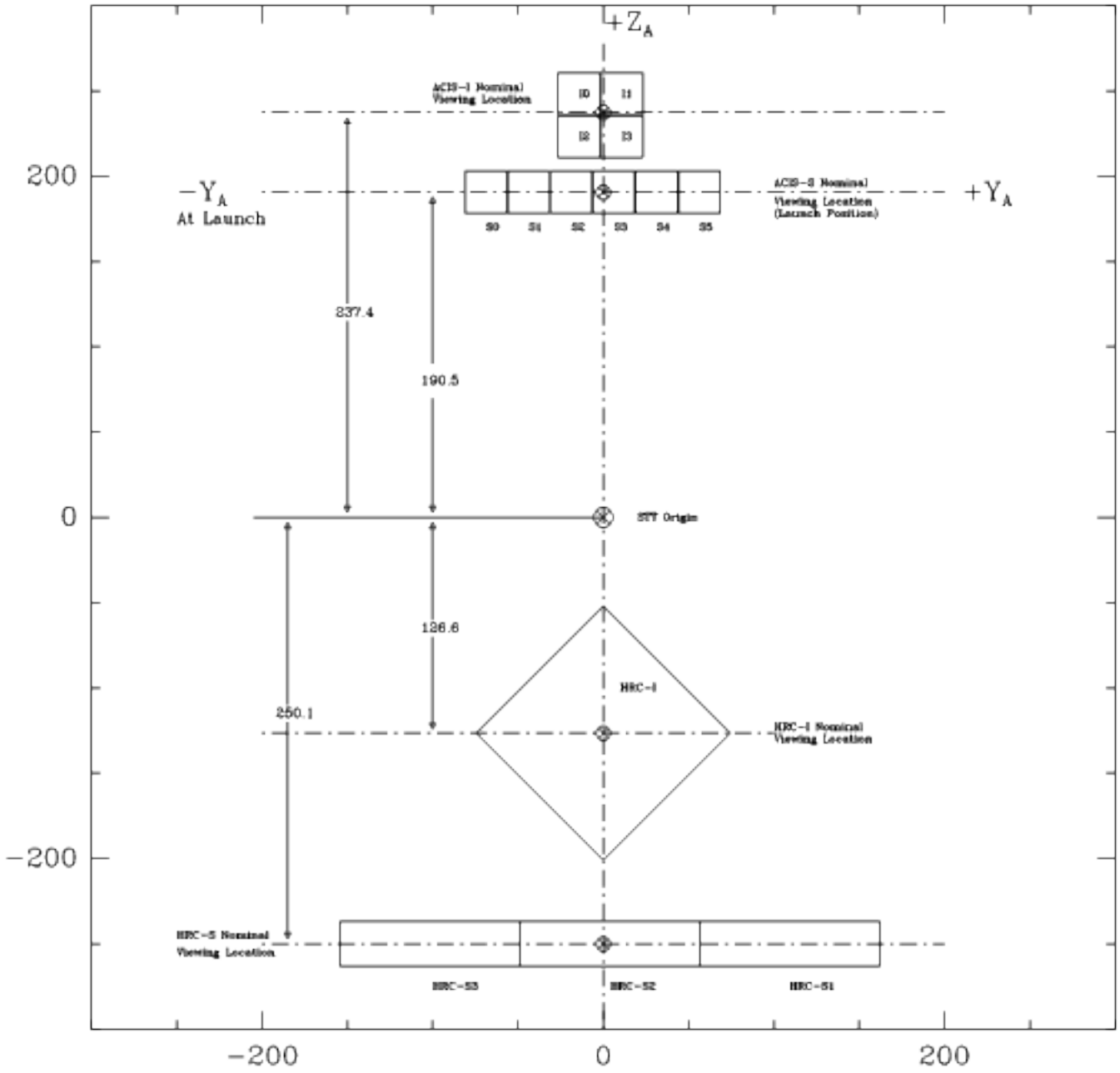

Figure 24: The AXAF SIM Translation Table, showing the flight focal plane instruments to scale. Distances are in mm. Coordinate system is STT.

4.3.1 Aimpoints

Several named default aimpoints are defined for the various AXAF instruments. The table below gives the STF coordinates of the instrument table origin for each of these aimpoints. Most observations will use one of these default aimpoints, but in general the SIM can be moved in X and Z to any aimpoint.

These 'aimpoints' are just the SIM locations used for typical observations. They don't imply that the optical axis of the telescope will fall at a particular location on the detector.

Table 14: SIM position offsets for nominal focus positions - values in CALDB 4.10.7 circa 2023

Values of $P_{STF}(\Sigma)$	
AI1 ACIS-I offset, I1 aimpoint	(-0.782, 0.0, -237.500)
AI2 ACIS-I offset, I3 aimpoint	(-0.782, 0.0, -233.592)
AS1 ACIS-S offset, S aimpoint	(-0.684, 0.0, -190.133)
HI1 HRC-I offset	(-1.040, 0.0, 126.985)
HS1 HRC-S offset, spec aimpoint	(-1.430, 0.0, 250.456)
HS2 HRC-S offset, imaging aimpoint	(-1.533, 0.0, 250.456)

4.3.2 Relative positions of instruments

The location of the origins of the LSI system for each instrument are given in STT coordinates in the table below, from the INSTRUMENTS section of the CALDB geometry file.

Table 15: Location of instrument origin on Translation Table

Values of $P_{STT}(S)$, i.e. offsets $S - \Sigma$	
ACIS origin	(0.684, 0.750, 236.552)
HRC-I origin	(1.040, 0.978, -132.028)
HRC-S origin	(1.533, 1.530, -251.437)

The CALALIGN file records STT coordinates for the aimpoints as shown in the following table. I am not sure how they are used.

Table 16: Location of instrument/aimpoint origin on Translation Table, CALALIGN

Values of $P_{STT}(S)$, i.e. offsets $S - \Sigma$	
ACIS-I origin	(0.0, 0.0, 237.40)
ACIS-S origin	(0.0, 0.0, 190.50)

HRC-I origin	(0.0, 0.0, -126.60)
HRC-S origin	(0.0, 0.0, 250.10)

4.4 The HRMA and the optical axis

4.4.1 HRMA to Aspect alignment

The telescope aspect camera (ACA) determines the celestial pointing direction of its own optical axis, imaging a star field. Simultaneously, a 'periscope' system superimposes an optical image of the focal plane on the field, showing the positions of a set of fiducial lights placed around the science instruments. Shifts of the fiducial lights relative to the stellar field reveal changes in ACA to STT alignment with time, which for Chandra occur at the arcsecond level during an observation. This measurement is called 'boresighting'.

The ACA is attached to the HRMA (which is fixed in MNC coordinates) and the HRMA is attached via the 'optical bench' main spacecraft tube to the SIM (fixed in STF coordinates, and related to STT coordinates via the SIM X,Y,Z values). We don't know from the aspect camera data alone whether an ACA-STT shift is caused by (a) an ACA-MNC shift, with the ACA moving relative to the HRMA mirror while the HRMA-SIM connection is rigid, or (b) an MNC-STT shift, with the ACA-HRMA connection rigid and the tube between the HRMA and the SIM bending. In case (a) the optical axis of the HRMA will remain aligned with the science instrument. In case (b) the optical axis of HRMA will move relative to the chip. X-ray sources won't move on the chip, but which X-ray source has the smallest PSF will change.

We identify the optical axis location through measurement of PSF sizes of sources in crowded fields; this calibration task is done on an approximately annual basis, in contrast to the boresighting done every few seconds. It was eventually concluded by P. Zhao and T. Aldcroft that Chandra exhibits case (a). The data processing pipeline adjusts the aspect solution pointing direction using the boresighting data on this assumption. (In earlier versions of the processing assumption (b) was used.)

In the aspect solution provided to the user, the file contains RA, DEC and ROLL values versus time, reflecting the inferred celestial position of the HRMA optical axis and the spacecraft roll angle around that axis. That celestial position corresponds on the detector to the center of the MSC frame (off-axis angle = 0, or for ACIS a DETX/Y value of 4096.5). By mapping MSC to CHIP one can then find the instantaneous celestial position on the chip of the axis, and thus the RA,Dec corresponding to any pixel.

4.4.2 A note on the optical axis aimpoint

When Chandra points at a particular RA, Dec, for a given SIM Z position of the instrument, the X-ray photons of an on-axis source will fall on a particular chip coordinate location on the detector. This location, often referred to as the aimpoint (but not to be confused with the standard SIM Z positions, also called aimpoints), does NOT appear explicitly anywhere in the processing system.

The center of the 'detector coordinate' system will always correspond to the optical axis, and by mapping these values - e.g. (4096.5, 4096.5) for ACIS - to the chip via the current SIM position

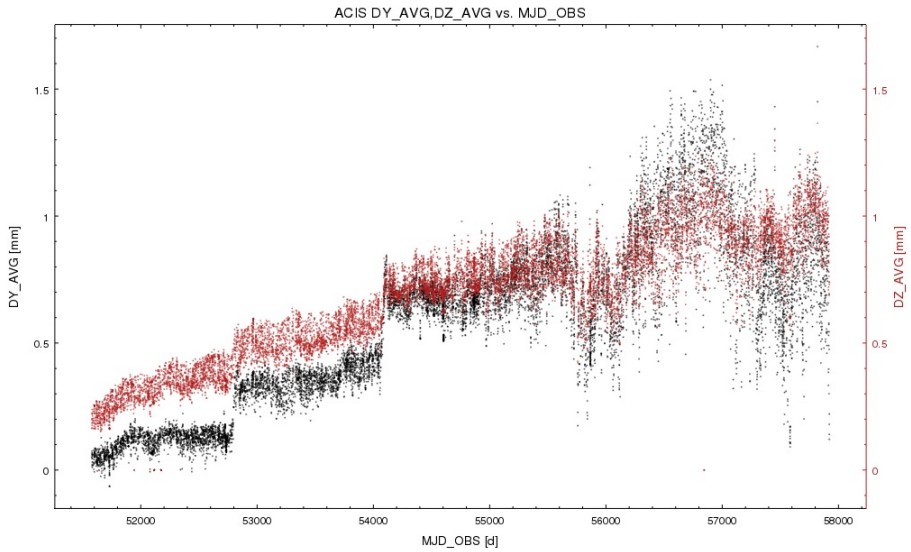

Figure 25: DY and DZ boresight offsets versus time for all ACIS data

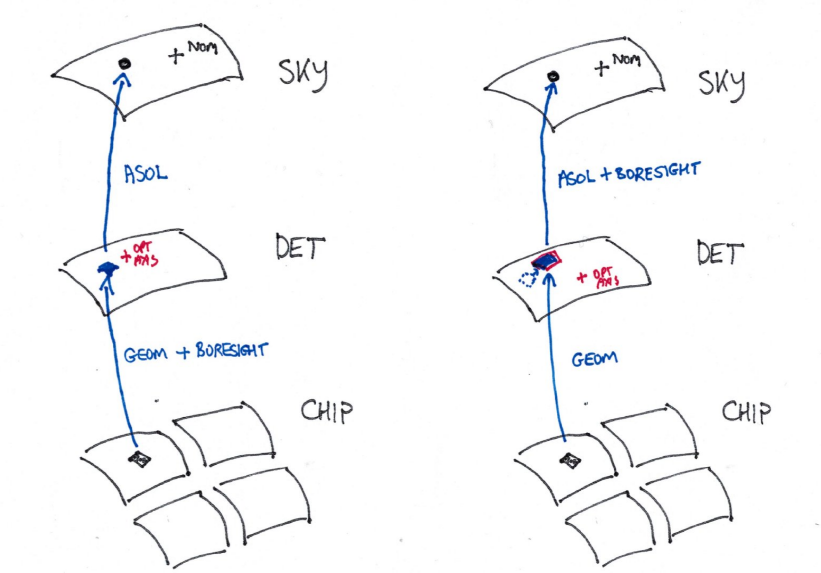

Figure 26: Comparison of old (left) and new (right) approaches. The boresight correction is now to be applied between the mirror (DET) plane and the sky plane instead of between the chip and mirror planes. As a result, DETX/DETY coordinates (and the corresponding off-axis angle) are changed, but the X/Y sky coordinates do not change.

you can find the aimpoint chip coordinates. (This can be done in software using the *pixlib* library, or by users with the *dmcoords* tool.)

Let us review the relevant coordinate systems:

- Each instrument (ACIS, HRC-I, HRC-S) has an LSI (Local Science Instrument) coordinate frame. The 3D positions of the chip corners are specified relative to this frame, and assumed fixed.
- The STT (SI Translation Table) system is a common frame for the translation table. The positions of the instruments on the table are assumed fixed and are specified in the INSTRUMENTS section of the CALDB geometry file, which gives a 3D origin of each LSI frame in STT coordinates. (There is also provision for an angular rotation, not currently used).
- The STF (SI Translation Frame) coordinate system is offset from the STT frame by an amount equal to the SIM X,Y,Z position, read from the observation file header. The STT-to-STF mapping allows us to capture the motion of the SIM to a given position (sometimes called 'aimpoint' but not to be confused with the optical axis). The origin of the STF frame is close to the optical axis.
- The DFC (Default Focal Coordinate) frame is centered on the optical axis of the telescope. The offset between the DFC and STF frames defines the position of the optical axis on the detectors. It is by default zero, is generally small, and is implemented as a time dependent correction using the time-resolved boresight DY, DZ values in the aspect solution file or, in the dmcoords tool, the time-independent DY_AVG, DZ_AVG header values in the event file.

The aspect pipeline produces boresight corrections DY, DZ versus time that represent relative motion between the aspect camera and the instrument table. Originally the L1 science instrument pipeline applied these offsets on the assumption that the aspect camera did not move relative to the HRMA optical axis, and (DY, DZ) represented optical axis-to-instrument (DFC to STF) relative motion. Analysis showed the contrary to be true: the optical axis has remained essentially fixed relative to the instruments. Therefore, the DY DZ corrections from the aspect pipeline are now applied to the aspect-camera-to-HRMA correction, affecting the RA and Dec values in the final aspect solution file (which are intended to be the RA and Dec of the HRMA axis). Further calibration could reveal a longer term change in the optical axis requiring a DFC to STF offset (DY_O, DZ_O); these values are currently set to zero.

The asp_offaxis_corr code converts a level 0 aspect solution to a level 1 aspect solution by:

- Taking the level 0 ASOL DY, DZ boresight offsets and applying them to level 0 ASOL RA, DEC values to create level 1 ASOL RA, DEC values.
- Setting the level 1 ASOL DY, DZ values to constant values DY_O, DZ_O (currently hardcoded to zero).

In the processing code (notably the generation of the level 1 and 2 event files), the detected CHIP event positions are mapped to the LSI frame using the positions of the chips, then to the STT frame using the instrument origins from the CALDB geometry file, then to the STF frame using the SIM position from the event header, and next to the DFC frame using the boresight offsets in the level 1 ASOL file. Then (using the fixed telescope focal length) the DFC coordinates are converted to off axis angle and azimuth and the corresponding pixel tangent plane DETX, DETY which allows users to visualize the events in off-axis-angle space. To adjust the location of optical axis one must therefore adjust the DFC to STF offsets by changing DY, DZ boresight offsets. However, fudging the STF to STT or STT to LSI offsets will effectively accomplish the same thing and may be more convenient in some contexts.

4.4.3 HRMA nodal coordinates

The conversion from STF (instrument compartment) to MNC (HRMA nodal) coordinates requires knowledge of the focal length, which is assumed to be 10065.512 mm as used in the CALALIGN calibration file.

$$\begin{pmatrix} X_{STF} \\ Y_{STF} \\ Z_{STF} \end{pmatrix} + \begin{pmatrix} f \\ 0 \\ 0 \end{pmatrix} = \begin{pmatrix} X_N \\ Y_N \\ Z_N \end{pmatrix} \tag{67}$$

In flight, the orientation of the SIM with respect to the HRMA is fixed. In an idealized nominal configuration, one of the SIs has its nominal focal point at the telescope focus. However, the SIM can be moved in X and Z so that the nominal focal point of the instrument and the telescope focus do not coincide, and this is the typical case for an actual observation.

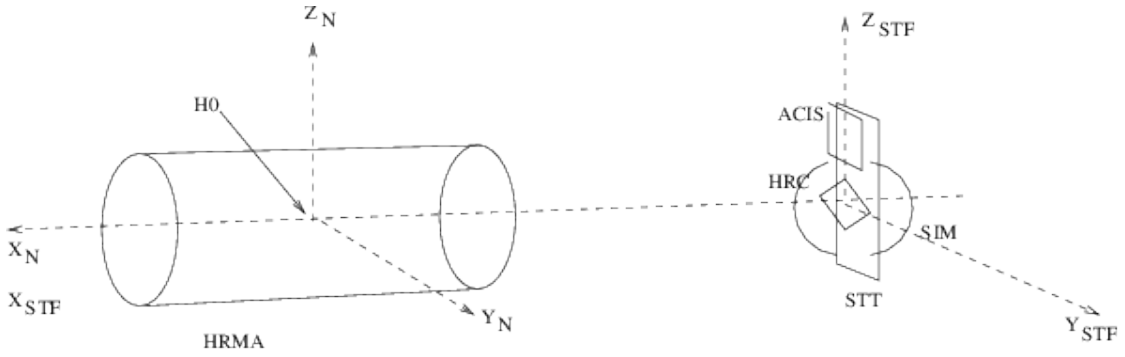

Figure 27: HRMA Nodal and STF Coordinates showing the on-orbit configuration. The SIM Transfer Table (STT) carrying the instruments moves along the Z_{STF} axis to select an instrument and along the X_{STF} axis to adjust focus.

4.4.4 Adjusting the effective optical axis position

In this section, intended mainly for those calibrating the telescope, I describe how to use the dmcoords tool and other ciao tasks to adjust the optical axis given an event file evt2.fits. The examples use ACIS data.

Note that the CALDB geometry file has the ACIS LSI origin as STT = (0.684, 0.750, 236.552) mm.

We can find the chip position of the optical axis for this observation by: (EXAMPLE 0)

```
dmcoords evt2.fits
dmcoords>: msc 0 0
(RA,Dec):    01:33:50.038     +30:40:10.50
(RA,Dec):        23.45850      30.66959 deg
THETA,PHI            0.0"          0.00 deg
(Logical):        4096.50       4096.50
SKY(X,Y):         4096.50       4096.50
DETX,DETY         4096.50       4096.50
CHIP ACIS-S3       220.73        532.20
TDET              4137.73       2234.20
```

The MSC coordinates are (off axis angle, azimuth) so "msc 0 0" sets the off-axis angle to zero - i.e. it chooses the optical axis - and then calculates other coordinates. Thus, for this data, the chip position of the optical axis is (220.7, 532.2) on ACIS-S3.

Important internal coordinate system values, not available to the user, are

```
DFC    -0.0023  0.0 0.0
STF    -0.0023  0.0 0.0
STT     0.6805  0.000  -190.1426
LSI    -0.0035 -0.7500  -46.4094
```

The center of chip S3 in this example has pixel coords (512.5, 512.5) which correspond to the following internal coordinates

```
DFC     0.0077 -6.9988  0.4687
STF     0.0077  6.9988 -0.4687
STT     0.6905  6.9988 189.6738
LSI     0.0065  6.2488 -46.8782
```

We can change the boresight values interactively in dmcoords: (Example 1)

```
dmcoords evt2.fits
dmcoords>: set sim/displace 0 4.2 1.3 0 0 0
```

```
dmcoords>: msc 0 0
(RA,Dec):    01:33:50.038     +30:40:10.50
(RA,Dec):        23.45850      30.66959 deg
THETA,PHI            0.0"          0.00 deg
(Logical):        4096.50       4096.50
SKY(X,Y):         4096.50       4096.50
DETX,DETY         4096.50       4096.50
CHIP ACIS-S3       395.86        586.30
TDET              4312.86       2288.30
```

The first three values in the 'set sim/displace' command are in mm and have, alas, the opposite sign to the DY, DZ values in ASOL. The chip position of the optical axis in this configuration is (395.9, 586.3) on ACIS-S3. This corresponds to internal coordinates

```
DFC   0.004  0.0         0.0
STF   0.004  4.200       1.300
STT   0.687  4.200     191.443
LSI   0.003  3.450     -45.109
```

The chip center in this configuration maps to internal coordinates

```
CHIP ACIS-S3       512.50        512.50
DFC   0.008  -2.799   1.769
STF   0.004  6.999  -0.469
STT   0.690  6.999 189.674
LSI   0.007  6.249 -46.878
```

Exactly the same results can be obtained by editing the event file header boresight keywords to

```
DY_AVG   = -4.20
DZ_AVG   = -1.30
```

or setting the DY, DZ values in the ASOL file to the same constant values for each row.

Another less rigorous approach is to edit the SIM_X, SIM_Y, SIM_Z values in the event header instead, or use the 'set sim' command in interactive dmcoords (Example 2)

```
dmcoords evt2.fits
dmcoords>: set sim  -0.6828 -4.2 -191.4426
dmcoords>: msc 0 0
(RA,Dec):    01:33:50.038     +30:40:10.50
(RA,Dec):        23.45850      30.66959 deg
```

```
THETA,PHI            0.0"          0.00 deg
(Logical):        4096.50       4096.50
SKY(X,Y):         4096.50       4096.50
DETX,DETY         4096.50       4096.50
CHIP ACIS-S3       395.86        586.30
TDET              4312.86       2288.30
```

This corresponds to internal coordinates

```
DFC   0.004  0.0       0.0
STF   0.004  0.0       0.0
STT   0.687  4.200   191.443
LSI   0.003  3.450   -45.109
```

Note that the final mapping between chip and off axis angle is the same as for example 1, but internal coordinate systems are different.

A further option (Example 3) is to add constant offsets to the ORIGIN values for each instrument in the INSTRUMENTS section of the CALDB geometry file. I changed the geometry file so that the ACIS ORIGIN changes from (0.684, 0.75, 236.5520) to (0.684, -3.45, 235.2520).

This results in

```
dmcoords evt2.fits
dmcoords>: msc 0 0
(RA,Dec):    01:33:50.039     +30:40:10.51
(RA,Dec):        23.45850      30.66959 deg
THETA,PHI            0.0"          0.00 deg
(Logical):        4096.50       4096.50
SKY(X,Y):         4096.50       4096.50
DETX,DETY         4096.50       4096.50
CHIP ACIS-S3       395.86        586.30
TDET              4312.86       2288.30
```

This results in internal coordinates

```
DFC   0.004  0.0     0.0
STF   0.004  0.000      0.000
STT   0.687  0.000    190.143
LSI   0.003  3.450    -45.109
```

Again, the final mapping between chip and off axis angle is the same as for example 1, but internal coordinate systems are different.

Example 1, either with 'set sim/displace', or using the event file boresight keywords, or - best - changing the aspect solution file DY, DZ columns - is the preferred approach.

4.4.5 Focal and Tangent plane systems

We define the following focal plane pixel systems, together with their usual purpose. The coordinate systems are defined in terms of their physical pixel size at the nominal flight focal length f = 10065.512 mm. The corresponding angular sizes are also given, but the actual angular size will be different for XRCF/HRMA and XRCF/TMA data.

We define systems for the nicely rounded pixel sizes and for the accurate actual pixel sizes. We've decided to use the mean actual pixel sizes for the flight system. Thus, the size of an HRC-I pixel at the nominal focal distance of 10065.512 mm is 0.132 arcseconds, so 0.132 arcseconds is defined as the FP-2.1 pixel size (even if the detector is moved well off focus). The HRC-S detector has a maximum linear extent of over 48500 pixels. When making sky coordinates for such a detector, we must define a square pixel plane (to allow for the roll angle). We choose a 65536 pixel sided plane, defined as FP-2.3. This plane has a total of 4.3 gigapixels, slightly more than can fit in a 4-byte signed integer. We therefore recommend not making full resolution full frame image files in this coordinate system.

Here are the current flight pixel systems:

System	Δ_{sp} (mm)	Δ_{s0} (arcsec)	t_x	t_y	FPX0, FPY0	Purpose
AXAF-FP-1.1	0.0240	0.492	+1	-1	4096.5	Flight ACIS, actual pixel
AXAF-FP-2.1	0.006429	0.132	+1	-1	16384.5	Flight HRC-I, actual pixel
AXAF-FP-2.3	0.006429	0.132	+1	-1	32768.5	Flight HRC-S

4.4.6 Angular systems

HRMA Left Handed Spherical Coordinates This system is used to express off-axis angles. We define HRMA Spherical Coordinates (r, θ_H, ϕ_H) in terms of HRMA nodal Cartesian coordinates as follows:

$$\begin{pmatrix} X_N \\ Y_N \\ Z_N \end{pmatrix} = \begin{pmatrix} +rcos\theta_H \\ -r\sin\theta_H\cos\phi_H \\ r\sin\theta_H\sin\phi_H \end{pmatrix} \tag{68}$$

The inverse is

$$\begin{aligned} r &= \sqrt{X_N^2 + Y_N^2 + Z_N^2} \\ \theta_H &= \cos^{-1}(X_N/r) \\ \phi_H &= \arg(-Y_N, Z_N) \end{aligned} \tag{69}$$

This coordinate system is also used for input to the XRCF Test Database; it is a LEFT HANDED coordinate system. The XRCF test database immediately converts these to pitch and yaw. The north pole of this system is the center of the forward aperture of the HRMA A0; θ_H measures the

off-axis angle of the incoming ray and ϕ_H measures its azimuth in the Y_N, Z_N plane such that for an observer at XRCF standing by the SI and looking at the XSS, $\phi_H = 0$ is to the left and $\phi_H = \pi/2$ is vertically downwards.

Then the forward aperture of the HRMA, A0, has HRMA nodal coordinates $(a, 0, 0)$ and HSC coordinates $(a, 0, 0)$. The focal point F of the HRMA has HRMA nodal coordinates $(-f, 0, 0)$ and HSC coordinates $(f, \pi, 0)$.

The coordinate system actually makes most sense when looking in the sky plane. Consider a source in the sky when roll angle is zero:

- *The FPX, FPY and X, Y axes are aligned.*
- *RA, Dec are parallel to -X, +Y. (since RA increases toward the left looking at the sky).*
- *The +X, +Y axes are parallel to -SCY, +SCZ. A photon from larger Dec and smaller RA than the field center comes from the +X, +Y direction. It enters the telescope from -SCY, +SCZ, and therefore has HSC coordinate azimuth between +0 and +90 deg. Thus, the HSC azimuth is just the conventional plane polar coordinate angle in the +FPX, +FPY tangent plane coordinate system.*
- *After passing through the (ideal) mirror origin, the photon leaves from +SCY, -SCZ and lands at +LSI Y, -LSI Z. (The HSC coordinates of the outgoing photon have azimuth between 180 and 270, and off axis angle between 90 and 270, but this is not normally of interest.)*

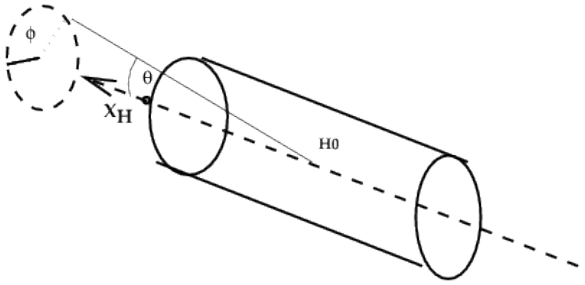

Figure 28: HRMA spherical coordinates

HRMA rotation coordinates (Pitch and Yaw) A third choice of pole is the $+Y_N$ axis, whose latitude-like coordinates α_z is called **yaw**, and whose azimuthal coordinate α_y is called **pitch**. The mapping between pitch and yaw coordinates and HRMA coordinates is

$$\begin{pmatrix} X_N \\ Y_N \\ Z_N \end{pmatrix} = \begin{pmatrix} +r\cos\alpha_z\cos\alpha_y \\ +r\sin\alpha_z \\ -r\cos\alpha_z\sin\alpha_y \end{pmatrix} \tag{70}$$

or

$$\begin{aligned} \alpha_z &= \sin^{-1}(Y_N/r) \\ \alpha_y &= \arg(X_N, -Z_N) \end{aligned} \tag{71}$$

The motivation for this coordinate system is its relationship to the commanded pitch and yaw of the HRMA at XRCF. We call the pitch and yaw coordinates of the XSS $\alpha_y(XSS) = \alpha_{y0}$ and $\alpha_z(XSS) = \alpha_{z0}$. To put the XSS at these coordinates, the HRMA must be yawed α_{z0} to the left and its aperture pitched α_{y0} downward.

HRMA Source coordinates HRMA Source Coordinates are related to the input coordinates used in the SAOSAC ray trace.

The HRMA Source Coordinate system (r, az, el) is a pseudo RA, Dec system that gives the 'sky' position of the source as seen by the HRMA. Unlike HRMA spherical coordinates, they have a pole at $-Z_N$ rather than X_N. The relationship between Source coordinates and HRMA nodal coordinates is:

$$\begin{pmatrix} X_N \\ Y_N \\ Z_N \end{pmatrix} = \begin{pmatrix} +r\cos\mathrm{el}\cos\mathrm{az} \\ -r\cos\mathrm{el}\sin\mathrm{az} \\ -r\sin\mathrm{el} \end{pmatrix} \tag{72}$$

Coordinates az =0, el = 0 refer to a source on the HRMA axis (center of the field of view); positive el gives a source above the HRMA axis (top of the field of view), while positive az gives a source to the left of the center of the field of view. The inverse function is

$$\begin{aligned} \mathrm{el} &= \sin^{-1}(-Z_N/r) \\ \mathrm{az} &= \arg(X_N, -Y_N) \end{aligned} \tag{73}$$

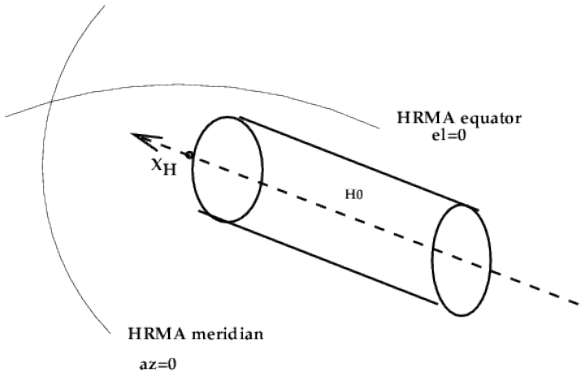

Figure 29: HRMA source coordinates

4.5 HETG and LETG

The Grating Node is on the optical axis at a distance R from the focus, where R is the diameter of the Rowland Circle. The nominal Rowland Circle diameter is quoted as 8650.0 mm [1], Appendix A, p. 11; 8633.69 mm [1], Drawing 301331, Sheet 3; and 8636.00 mm [3]. However View F on the same drawing 301331 shows the Rowland circle intercepting the X axis at $X_A = 372.116$ corresponding to R = 8643.11 mm. This is an error caused by confusing H0 and H1 when measuring the location of the OTG origin.

Post-flight calibration has led to R values of 8632.48 mm for HETG and 8637.0 mm for LETG.

The MNC coordinates of the Grating Node ***G0*** in flight are

$$\begin{pmatrix} X_N(G0) \\ Y_N(G0) \\ Z_N(G0) \end{pmatrix} = \begin{pmatrix} -1431.81 \\ 0 \\ 0 \end{pmatrix} \tag{74}$$

(The exact value was different at XRCF.) We use the same physical pixel size as for the detector systems, which correspond to somewhat different angular sizes than the imaging case because we are measuring angles from G rather than H0. However, in the case of ACIS, we hope to get extra resolution by using the sub-pixel dither of the detector relative to the sky coordinate zero order position. So, in the GDP-1.1 system we have chosen the GDP pixel size for ACIS and HRC to be the same 6 micron value. (In an earlier version of this memo, the GDP-1.0 system was described with 24 micron ACIS GDP pixel sizes. That system was never implemented.)

What is the extent of the GDP coordinate system? In the case of HRC-S, our worst case is a zero order at an extreme end of the 3-chip array. In that case, you could be as many as 49152 pixels down the dispersion coordinate. Such a zero order position is such a pathological case that we have decided not to build our definitions around it. A normal case would be a zero order in the center, with dispersion coordinates up to plus or minus 25000 pixels or so. As a compromise to support most off axis cases, we adopt pixels running from 1 to 65536 in the dispersion direction, giving 32768 pixels on either side of zero order. In the cross dispersion direction, with HRC-I as the detector, we might have photons up to 16384 pixels from the zero order in principle, and 8192 even if the source is centered in the detector. For ACIS, the extreme range is 32678 super-resolved pixels in the dispersion direction and 24800 pixels in the cross dispersion direction. For both ACIS and HRC, the GDP-1.1 system is sized to be 65536 pixels in the dispersion direction and 32678 pixels in the cross dispersion direction, with the zero order position at (32768.5, 16384.5). However, we recommend that in normal use the 32768 x 4096 subarray extending from (16384,14336) to (49152,18432) be used. This subarray is defined as AXAF-GDP-1.2; it has the same pixel size as GDP-1.1.

Table 18: GDC pixel image centers

Instrument	System	GDX0, GDY0	Image size

ACIS,HRC	GDP-1.1	32768.5, 16384.5	65536 x 32768
ACIS,HRC	GDP-1.2	16384.5, 2048.5	32768 x 4096

Table 19: GDP Pixel Sizes (assuming flight Rowland radius)

Instrument	System	Size at Focal Plane Δ_p, Δ_{gp} (mm)	Angular Size $\Delta_g s$ (arcsec)
ACIS	GDP	0.006430	0.154
HRC	GDP	0.006430	0.154

The average grating periods for the three gratings are given in the table below.

Table 20: Grating properties

Instrument	P	α_G (deg)	Rowland radius
HETG	2000.81$\mathring{A}$	-5.2050	8632.48
METG	4001.95$\mathring{A}$	-4.7550	8632.48
LETG	9912.16$\mathring{A}$	-0.0167	8637.00

5 Appendices

5.1 Coordinate system identifiers

We assigned identifier strings for version control of the coordinate systems. In practice we haven't made use of these strings much if at all. They are listed here for historical reference.

Identifier	Abbreviation	Name of system	Variables	Notes
ASC-CHIP-1.0	CPC	Chip Physical	Inst. ID,	Single chip
ASC-FP-LSI-1.0	LSI	Local SI	Inst. ID	Focal plane, offset uncorrected
ASC-FP-STT-1.0	STT	SI Translation Table	Pixel size	Focal plane, offset uncorrected
ASC-FP-STF-1.0	STF	SI Translation Frame	Pixel size	Focal plane, alignment uncorrected
ASC-FP-FSC-1.0	FC	Focus Coordinates	Pixel size	Focal plane
ASC-FP-FSC-1.0	MNC	Mirror Nodal	Pixel size	Focal plane
ASC-FP-FSC-1.0	FSC	Focal Surface	Pixel size	Focal plane
ASC-TP-MSC-1.0	MNC	Mirror Nodal	Pixel size	Tangent plane
ASC-TP-MSC-1.0	MSC	Mirror Spherical	Pixel size	Tangent plane
ASC-SKY-1.0	CEL	Celestial	Pixel size	Aspect applied
ASC-TP-MSC-1.0	PTP	Physical Tangent Plane	Pixel size	Tangent Plane 3D
ASC-SKY-1.0	PSP	Physical Sky Plane	Pixel size	Sky Plane 3D
ASC-TDET-1.0	TDET	TDET	TDETX, TDETY	Abstract system, obsolete
AXAF-ACIS-1.0	CHIP	ACIS Chip	CHIPX, CHIPY	In standard event file
AXAF-ACIS-2.2	TDET	ACIS TDET	TDETX, TDETY	Largely obsolete
AXAF-ACIS-3.0	-	ACIS Readout	XREAD, YREAD	Internal to instrument telemetry?
AXAF-ACIS-4.0	-	Window Chip	WX, WY	In ACIS window mode telemetry
AXAF-HRC-1.0	CHIP	HRC Chip	CHIPX, CHIPY	Retired (see v3.0 of document)
AXAF-HRC-1.1	CHIP	HRC Chip	CHIPX, CHIPY	In standard event file
AXAF-HRC-2.3I	TDET	HRC-I TDET	TDETX, TDETY	Largely obsolete
AXAF-HRC-2.6S	TDET	HRC-S TDET	TDETX, TDETY	Largely obsolete
AXAF-HRC-6.0	RAW	HRC Tap system		Internal use
AXAF-FP-1.1	SKY	ACIS Focal plane	FPX, FPY	Used for SKY coords
AXAF-FP-2.1	SKY	HRC-I Focal plane	FPX, FPY	Used for SKY coords
AXAF-FP-2.3	SKY	HRC-S Focal plane	FPX, FPY	Used for SKY coords
AXAF-STT-1.0	STT	SIM Translation coords	STT X Y Z	Internal calcs only
AXAF-HSC-1.1	(MSC)	Mirror Spherical	Theta, Phi	HRMA mirror spherical (left-handed)
AXAF-HSC-1.2	MSC	Mirror Spherical	Theta, Phi	Right-handed systen, retired
AXAF-HSC-2.0	-	Source coordinates		Left-handed system, retired
AXAF-HSC-2.1	-	Source coordinates		Right-handed system, Not used in practice
AXAF-HSC-3.0	-	HRMA pitch and yaw		Used for XRCF data

5.2 More conventions

Vector and coordinate notation

A bold face symbol e.g. $\boldsymbol{B}$ denotes a point in 3D space. The notation $Y_A(\boldsymbol{B})$ denotes the Y coordinate of point $\boldsymbol{B}$ in the 3-dimensional Cartesian coordinate system A. When we refer to a point as an argument in this way we usually get lazy and omit the boldface, e.g. $Y_A(B)$. The notation $P_A(B)$ denotes the triple $(X_A(B), Y_A(B), Z_A(B))$, i.e. the coordinates of $\boldsymbol{B}$ in the A coordinate system. (P is not in boldface since it is not a vector - it is in a specific coordinate system.)

Rotation and translation of Cartesian systems

We define an Euler rotation $\mathrm{Rot}(\phi_E, \theta_E, \psi_E)$ of a Cartesian system X,Y,Z to be the product of three rotations

$$\mathrm{Rot}(\phi_E, \theta_E, \psi_E) = \mathrm{Rot}_1(Z, \psi_E)\mathrm{Rot}_1(Y, \theta_E)\mathrm{Rot}_1(Z, \phi_E) \tag{75}$$

where the rotations apply to the successively rotated axes from right to left in the usual sense of matrix multiplication,

The general transformation from a cartesian system A to a system B involves a scaling, a translation, and a rotation. This may be described by seven numbers: the scale factor K_{AB} (choice of units), the position vector $P_B(A0) = (X_B(A0), Y_B(A0), Z_B(A0))$ of the origin of A in the B system, and the three Euler angles ϕ_E, θ_E, ψ_E of the rotation R(A,B) from A to B,

$$\begin{aligned} R(A,B) &= Rot(\phi_E, \theta_E, \psi_E) \\ &= \begin{pmatrix} \cos\phi_E \cos\theta_E \cos\psi_E - \sin\phi_E \sin\psi_E & \sin\phi_E \cos\theta_E \cos\psi_E + \cos\phi_E \sin\psi_E & -\sin\theta_E \cos\psi_E \\ -\cos\phi_E \cos\theta_E \sin\psi_E - \sin\phi_E \cos\psi_E & -\sin\phi_E \cos\theta_E \sin\psi_E + \cos\phi_E \cos\psi_E & \sin\theta_E \sin\psi_E \\ \cos\phi_E \sin\theta_E & \sin\phi_E \sin\theta_E & \cos\theta_E \end{pmatrix} \end{aligned} \tag{76}$$

Then coordinates of a general point G

$$P_A(G) = (X_A(G), Y_A(G), Z_A(G)) \tag{77}$$

may be converted to

$$P_B(G) = (X_B(G), Y_B(G), Z_B(G)) \tag{78}$$

using the formula

$$\boxed{P_B(G) = R(A,B) K_{AB} P_A(G) + P_B(A0)} \tag{79}$$

If

$$R(A,B) = Rot(\phi_E, \theta_E, \psi_E) \tag{80}$$

then

$$R(B,A) = Rot(\pi - \psi_E, \theta_E, \pi - \phi_E). \tag{81}$$

Further, if C is related to B by reflection about the X axis, i.e. $Y_C = -Y_B, Z_C = -Z_B$ then

$$R(A,C) = Rot(\phi_E, \pi + \theta_E, \pi - \psi_E). \tag{82}$$

Spherical polar coordinates

We also use spherical polar coordinate systems. The WCS paradigm describes general rotations of a spherical polar coordinate system. We define the native cartesian axes X,Y,Z of a spherical polar system (r, θ, ϕ) by the equation

$$(X, Y, Z) = r\mathcal{S}(\theta, \phi) = (r\cos\phi\sin\theta, r\sin\phi\sin\theta, r\cos\theta) \tag{83}$$

so that the north pole is through the positive Z axis and the azimuth is zero along the positive X axis and 90 degrees along the positive Y axis. Any other choice of spherical coordinates (r, θ', ϕ') may be defined by specifying the Euler rotation matrix which rotates the corresponding native systems into each other.

One may derived:

$$\boxed{\begin{aligned} \theta' &= \cos^{-1}\left(\cos\theta_E \cos\theta + \sin\theta_E \sin\theta \cos(\phi - \phi_E)\right) \\ \phi' &= \arg\left(\cos\theta_E \sin\theta \cos(\phi - \phi_E) - \sin\theta_E \cos\theta, \sin\theta \sin(\phi - \phi_E)\right) - \psi_E \end{aligned}} \tag{84}$$

References

[1] TRW IF1-20, Observatory to Science Instrument ICD, 11 Jan 1996.

[2] TRW SE30, AXAF-I System Alignment Plan, D17388, 11 Jan 1996.

[3] AXAF Transmission Grating Diffraction Coordinates, ASC Memo, D.P. Huenemorder, 2 Apr 1996.

[4] EQ7-002 Rev D.